

Enhancer architecture-dependent multilayered transcriptional regulation orchestrates RA signaling-induced early lineage differentiation of ESCs

Guangsong Su^{1,†}, Wenbin Wang^{1,†}, Xueyuan Zhao^{1,†}, Jun Chen¹, Jian Zheng¹, Man Liu¹, Jinfang Bi¹, Dianhao Guo¹, Bohan Chen¹, Zhongfang Zhao¹, Jiandang Shi¹, Lei Zhang^{1,*} and Wange Lu^{1,2,*}

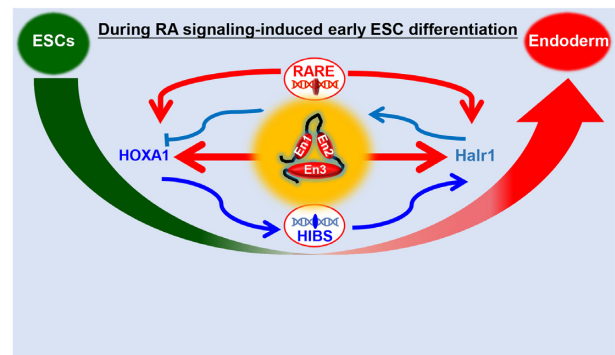
¹College of Life Sciences, Nankai University, 94 Weijin Road, 300071 Tianjin City, China and ²State Key Laboratory of Medicinal Chemical Biology, Nankai University, 94 Weijin Road, 300071 Tianjin City, China

Received July 28, 2021; Revised September 16, 2021; Editorial Decision October 09, 2021; Accepted October 12, 2021

ABSTRACT

Signaling pathway-driven target gene transcription is critical for fate determination of embryonic stem cells (ESCs), but enhancer-dependent transcriptional regulation in these processes remains poorly understood. Here, we report enhancer architecture-dependent multilayered transcriptional regulation at the *Halr1–Hoxa1* locus that orchestrates retinoic acid (RA) signaling-induced early lineage differentiation of ESCs. We show that both homeobox A1 (*Hoxa1*) and *Hoxa* adjacent long non-coding RNA 1 (*Halr1*) are identified as direct downstream targets of RA signaling and regulated by RARA/RXRA via RA response elements (RAREs). Chromosome conformation capture-based screens indicate that RA signaling promotes enhancer interactions essential for *Hoxa1* and *Halr1* expression and mesoderm differentiation of ESCs. Furthermore, the results also show that HOXA1 promotes expression of *Halr1* through binding to enhancer; conversely, loss of *Halr1* enhances interaction between *Hoxa1* chromatin and four distal enhancers but weakens interaction with chromatin inside the *HoxA* cluster, leading to RA signaling-induced *Hoxa1* overactivation and enhanced endoderm differentiation. These findings reveal complex transcriptional regulation involving synergistic regulation by enhancers, transcription factors and lncRNA. This work provides new insight into intrinsic molecular mechanisms underlying ESC fate determination during RA signaling-induced early differentiation.

GRAPHICAL ABSTRACT



INTRODUCTION

ESCs can undergo unlimited self-renewal and proliferation, while maintaining the potential to differentiate into different germ layers, activities requiring precise control of gene expression (1,2). Recent studies indicate that in addition to promoters, there are many other types of functional DNA elements such as enhancers, insulators, silencers and transposable elements that control the precise expression of gene in ESCs (3–6). Enhancers also reportedly show significant cell-type specificity during ESC lineage differentiation stimulated by different signaling factors, while results obtained by chromosome conformation capture also reveal significant changes in high-order chromatin structure during these processes (7,8). Although enhancers regulate expression of master transcription factors (TFs) through long-range chromatin interactions to coordinate embryonic development (9–11), the precise mechanisms underlying the regulation of enhancer in ESC lineage differentiation remain largely unclear.

*To whom correspondence should be addressed. Tel: +86 22 23503617; Fax: +86 22 23503617; Email: wanglv@gmail.com
Correspondence may also be addressed to Lei Zhang. Tel: +86 22 23503617; Fax: +86 22 23503617; Email: joyleizhang@nankai.edu.cn
†The authors wish it to be known that, in their opinion, the first three authors should be regarded as Joint First Authors.

RA signaling is essential for mammalian development and functions in embryogenesis, immunogenesis, hematopoiesis and skeletogenesis (12,13). Abnormal RA signaling underlies numerous disease states, including tumorigenesis (12,14,15). ESCs rapidly differentiate in response to RA signaling, a process requiring transcriptional regulation by the RA receptor RXR/RAR (16,17). Recent studies show that RA signaling induces neural differentiation of ESCs, with *HOXA1* playing a central transcriptional role in this process (18–21) and CTCF organizing chromatin interactions (22–24). However, early stages of ESC differentiation induced by RA signaling are reportedly characterized by endodermal differentiation marked by significantly high expression of endodermal master control genes *Gata4*, *Sox17* and *Gata6* (25,26). These findings suggest that ESCs may undergo multi-lineage differentiation in response to RA signaling, and that the underlying molecular regulatory mechanisms are unknown.

We and others have found that several enhancers and CTCF binding elements (CBEs) at the *Halr1–Hoxa1* locus play important regulatory roles during RA signaling-induced ESC differentiation (23,26–29). In addition, the long non-coding RNA (lncRNA) *Halr1* also reportedly regulates *HoxA* cluster gene expression by orchestrating enhancer interactions under RA-induced early ESC differentiation (27,29). However, regulatory relationships between enhancers, CBEs, lncRNAs and *HoxA* following RA induction of early ESC differentiation remain unknown. Considering that all these elements are present at the *Halr1–Hoxa1* locus, analyses of their activity in this context may provide an excellent model to define mechanisms involved in RA signaling-induced early ESC differentiation.

Here, using the *Halr1–Hoxa1* locus as a model, we conducted various analyses of ESC differentiation and showed that RA signaling significantly induced differentiation towards ectoderm and endoderm lineages and that *Halr1* and *Hoxa1* were significantly activated in this process. We also identified *Halr1* and *Hoxa1* as direct downstream targets of RA signaling and found that proper *Halr1* and *Hoxa1* expression is necessary for RA-dependent induction of endodermal ESC differentiation. Moreover, multiple enhancers at the *Halr1–Hoxa1* locus were required for RA signaling to induce *Halr1* and *Hoxa1* expression and mesendoderm differentiation. We also observed reciprocal regulation between *Hoxa1* and *Halr1*: *HOXA1* promoted *Halr1* expression by binding to enhancer regions, while *Halr1* repressed *Hoxa1* expression by coordinating interactions of multiple enhancers with *Hoxa1* chromatin. Finally, we identified a subset of genes regulated by *HOXA1* associated with endoderm development. Overall, these findings reveal a new mechanism for RA signaling-induced early lineage differentiation of ESCs and provide a new perspective on ESC fate decisions.

MATERIALS AND METHODS

ESCs culture

Mouse ESCs E14 were cultured in undifferentiated condition as previously described (23). Briefly, ESCs were grown in culture dishes coated with 0.1% gelatin (Sigma) in Dulbecco's modified Eagle's medium (DMEM, Gibco) supple-

mented with 15% fetal bovine serum (FBS, AusGeneX), 1× nonessential amino acids (100×, Gibco), 1× L-glutamate (100×, Gibco), 1× penicillin–streptomycin (100×, Gibco), 50 μM β-mercaptoethanol (Sigma), 10 ng/ml LIF (ES-GRO), 1 μM PD0325901 (MedChemExpress) and 3 μM CHIR99021 (MedChemExpress). The medium was replaced every 1–2 days. ESCs were maintained at 37°C in a 5% CO₂ incubator.

Adherent differentiation of ESCs

ESC differentiation was carried out as previously reported (23,26). ESCs were gently washed with 1× phosphate buffer saline solution (PBS, Solarbio), dissociated, and plated at an appropriate density on gelatin-coated plates in LIF/2i withdrawal medium or medium supplemented with 2 μM RA (Solarbio). The differentiated culture mediums were replaced every day.

Embryoid bodies (EBs) formation

For EB formation, 10⁶ ESCs were plated on non-adherent 10 cm plates in LIF/2i withdrawal medium. EBs were harvested using TRIzol reagent (Invitrogen) every day. RNA was prepared, and qRT-PCR was performed as described previously (26,30).

Alkaline phosphatase (AP) staining analysis

ESCs were plated at low density in 12-well plates coated with gelatin for 3 days, washed twice with PBS, and then incubated with reagents from the AP Staining kit (System Biosciences) following the manufacturer's instructions. Digital images were taken using an Olympus Inverted Fluorescence Microscope (26).

RNA extraction, cDNA synthesis and quantitative Real-Time PCR (qRT-PCR)

Total RNA was extracted from differentiated or undifferentiated ESCs using TRIzol Reagent (Life Technologies). cDNA synthesis was performed using a PrimerScript™ RT reagent Kit with gDNA Eraser (TaKaRa) according to the manufacturer's instructions. PCR reactions were performed using Hieff™qPCR SYBR Green Master Mix (YEASEN) and a BioRad CFX Connect Real-Time system. PCR cycling conditions were as previously reported: 95°C for 5 min, 40 cycles of 95°C for 15 s, 60°C for 15 s and 72°C for 30 s. We then constructed a melting curve of amplified DNA (23,26). Target gene values were normalized to *Gapdh* expression and the experimental control using $\Delta\Delta C_t$ methods (31). Primer sequences used in this study are shown in Supplementary Table S1.

Construction of stably transduced ESC lines

Full-length coding sequences (CDSs) of *Rara*, *Rxra* and *Hoxa1* were synthesized at GENEWIZ and inserted into the FLAG-tag vector using NheI and NotI sites. ESCs were transfected with the overexpression vectors using Lipofectamine 3000 (Life Technologies) and then 24 h later were

treated with medium containing 5 μ M puromycin (MCE) until stably-transduced cells were harvested. qRT-PCR and western blot (WB) were used to identify overexpression cell lines (26). Full-length CDSs of *Rara*, *Rxra* and *Hoxa1* are shown in Supplementary Table S2.

Western blot analysis in ESCs

Protein was extracted using RIPA lysis buffer (Strong, YEASEN) and electrophoresis was performed using a PAGE Gel Quick Preparation Kit (10%, YEASEN) following the manufacturer's instructions. WB was carried out with the following antibodies: (primary) RARA (Invitrogen, #MA1-810A, 1:1000), RXRA (Invitrogen, #433900, 1:1000), HOXA1 (Invitrogen, #PA5-68809, 1:1000), FLAG (Beyotime, #AF-0036, 1:1000) and GAPDH (Santa Cruz, #SC-365062, 1:2000), and then HRP-linked secondary antibodies (Sungene Biotech). HRP activity was detected using Luminol HRP Substrate (Millipore). Digital images were taken using an automatic chemiluminescence imaging analysis system (Tanon) (6,26,32,33).

CRISPR/Cas9-mediated genome editing in ESCs

CRISPR/Cas9-mediated knockout was performed using published protocols (23,26,34). Briefly, target-specific guide RNAs (sgRNAs) were designed using an online tool (<http://chopchop.cbu.uib.no/>). sgRNAs of the appropriate site and score were selected and sgRNAs were cloned into a Cas9-puro vector using the Bsmbl site. sgRNA sequences are shown in Supplementary Table S3.

For enhancer and TF binding site knockout cells, ESCs were transfected with two sgRNA plasmids using Lipofectamine 3000 (Life Technologies), and 24 h later, cells were treated with 5 μ M puromycin (MCE) for 24 h and then cultured in a medium without puromycin for another 5–7 days. Individual colonies were picked and validated by genomic DNA PCR or subsequent Sanger DNA sequencing. Enhancer knockout lines En1-KO, En2-KO, En3-KO and En1/2/3-KO were reported in our previous study (23). For coding gene knockouts, sgRNAs were designed at both ends of the gene CDS based on a previous report (21). Successful knockout lines were validated by genomic DNA PCR, qRT-PCR and WB. For lncRNA knockouts, sgRNAs were designed at the promoter region based on a previous report (27). Successful knockout lines were validated by genomic DNA PCR and qRT-PCR. PCR primers used for genotyping are listed in Supplementary Table S4.

Chromosome conformation capture (Capture-C) assay and data analysis

Probes used for Capture-C assay were designed using an online tool (<http://apps.molbiol.ox.ac.uk/CaptureC/cgi-bin/CapSequm.cgi>). Probe sequences are listed in Supplementary Table S5. Capture-C libraries were prepared as described (23,26,35,36). Briefly, undifferentiated or RA-induced differentiated ESCs were fixed with 1% (vol/vol) formaldehyde for 10 min at room temperature, quenched with 125 mM glycine in PBS, and then lysed in cold lysis buffer [10 mM Tris-HCl, pH 7.5, 10 mM NaCl, 5 mM

MgCl₂, 0.1 mM EGTA, 0.2% NP-40, 1 \times complete protease inhibitor cocktail (Roche)]. Chromatin was digested with DpnII (New England Biolabs) at 37°C overnight. Fragments were then diluted and ligated with T4 DNA ligase (Takara) at 16°C overnight. Cross-linking was reversed by overnight incubation at 60°C with proteinase K (Biolone). Then 3C libraries were purified by phenol–chloroform followed by chloroform extraction and ethanol-precipitated at –80°C overnight. Sequencing libraries were prepared from 10 μ g of the 3C library by sonication to an average size of 200–300 bp and indexed using NEBnext reagents (New England Biolabs), according to the manufacturer's protocol. Enrichment of 2 μ g of an indexed library incubated with 3 μ M of a pool of biotinylated oligonucleotides was performed using the SeqCap EZ Hybridization reagent kit (Roche/NimbleGen), following the manufacturer's instructions. Two rounds of capture employing 48–72 h and 24 h hybridizations, respectively, were used. Correct library sizes were confirmed by agarose gel electrophoresis, and DNA concentration was determined using a Qubit 2.0 Fluorometer (Thermo Fisher Scientific). All sequencing was performed on Hi-Seq 2500 platforms using paired 150 bp protocols (Illumina).

Capture-C data were analyzed as previously described methods (23,26,35,36). Briefly, clean paired-end reads were reconstructed into single reads using FLASH (37). After *in silico* DpnII digestion using the DpnII2E.pl script, reads were mapped back to the mm10 mouse genome using Bowtie1. Finally, chimeric reads containing captured reads and Capture-Reporter reads were analyzed using CC-analyser3.pl. Results were visualized using the Integrated Genome Browser (IGV) (38) and an online tool (<https://epgg-test.wustl.edu/browser/>) (39).

Eukaryotic cognate transcriptome sequencing (RNA-seq) and data analysis

RNA-seq was performed as reported (23,26). Briefly, ESCs were lysed with Trizol reagent (Life Technologies), and RNA was extracted based on the manufacturer's instructions. RNA was sequenced by the Novogene. Clean reads were mapped to the Ensemble mm10 mouse genome using Hisat2 with default parameters. Gene reads were counted by Htseq (40). Fold changes (FC) were computed as a log₂ ratio of normalized reads per gene using the DEseq2 R package (41). Gene expression with |log₂ FC| \geq 1 (FDR < 0.05) was considered significantly altered. Heatmaps were drawn using the heatmap.2 function or Microsoft Excel 97-2003. At least two biological replicates were analyzed for each experimental condition.

Gene ontology (GO) analysis

GO analyses were performed using the following online tools: Metascape (<http://metascape.org/gp/index.html#/main/step1>) (42) and DAVID Functional Annotation Bioinformatics Microarray Analysis tool (<http://david.abcc.ncifcrf.gov/>) (43). Briefly, differential genes (FC \geq 2, FDR < 0.5) were loaded into the analysis module as instructed by the tools, then the mouse was selected as the species for GO analysis to obtain the final output.

Gene set enrichment analysis (GSEA)

GSEA analysis was carried out using an online tool (<https://www.gsea-msigdb.org/gsea/index.jsp>) as reported (44,45). Gene sets of embryonic skeletal system morphogenesis and stem cell population maintenance were obtained from the KEGG database (<https://www.genome.jp/kegg/>) (46).

Data set availability

DNA-seq and RNA-seq data have been deposited in the NCBI Gene Expression Omnibus (GEO, <https://www.ncbi.nlm.nih.gov/geo/>) under accession number GSE169058. Previously published datasets used in this study are shown in Supplementary Table S6. These published data sets were downloaded and analyzed using online tools (<http://cistrome.org/db/#/>, <http://promoter.bx.psu.edu/hi-c/> and <https://www.ncbi.nlm.nih.gov/geo/>) (47–49).

Statistical analysis

Data were analyzed by the unpaired Student's *t*-test (two-tailed) unless otherwise specified. Statistically significant *P*-values are indicated in Figure legends as follows: * *P* < 0.05, ** *P* < 0.01.

RESULTS

Characterization of RA signaling-induced early lineage differentiation of ESCs

To analyze characteristics of RA-induced differentiation of ESCs, we employed three commonly used ESC differentiation protocols: spontaneous differentiation following LIF/2i removal, differentiation induced by RA after LIF/2i removal, and embryoid body (EB) differentiation (Figure 1A). As differentiation proceeded, differentiated cells showed greater cell morphological differences compared to undifferentiated ESCs (Figure 1B and C). Pluripotency marker genes and germ layer marker genes were used to identify ESC differentiation status (23,50), qRT-PCR results showed that *Nanog* and *Klf4* levels decreased with time in all three protocols, and RA-induced ESC differentiation resulted in significantly higher expression of ectodermal (*Sox1* and *Pax6*) and endodermal (*Gata4*, *Gata6*, *Foxa2* and *Sox17*) genes, compared with the other differentiation schemes (Figure 1D), suggesting that RA-induced ESCs' early differentiation has the significant ectodermal and endodermal profile.

To further assess the global view of gene expression changes, we performed transcriptome sequencing (RNA-seq) at day one after RA treatment. At that time point, we observed 3070 up-regulated and 3303 down-regulated genes compared to undifferentiated ESCs (Supplementary Figure S1A). Further analysis of germ layer gene expression revealed significant up-regulation of genes associated with the ectoderm, trophoderm and endoderm, with the greatest up-regulation in endodermal genes (Supplementary Figure S1B and C). GO analysis also showed enrichment of biological processes associated with multicellular organism development, cell differentiation, endoderm formation and cellu-

lar responses to RA (Supplementary Figure S1D; Supplementary Table S7). Taken together, these data suggest that RA signaling significantly induces early ESC differentiation into endoderm and ectoderm.

Hoxa1 and *Halr1* are direct downstream target genes of RA signaling

To explore the expression patterns of *Hoxa1* and *Halr1*, we next evaluated their transcript levels in various ESC differentiation models. qRT-PCR results showed that *Hoxa1* and *Halr1* were more robustly expressed following RA-induced ESC differentiation relative to other differentiation systems (Figure 1D). Upon analysis of the RNA-seq data, we found that *Hoxa1* and *Halr1* were significantly enriched in the biological processes associated with cellular response to RA (Supplementary Figure S1D and E). In addition, we also found that *Halr1* transcript levels peaked at day one of differentiation (Supplementary Figure S2A and B). These results suggest that RA signaling can specifically and significantly activate the expression of *Hoxa1* and *Halr1* during early ESC differentiation.

The transcriptional activation ability of RA signaling is dependent on RA receptors such as RARA and RXRA (16). Thus, we asked whether *Hoxa1* and *Halr1* expression depended on RARA and RXRA. To do so, we first analyzed ChIP-seq data for RARA/RXRA and found that RA induced a significant co-binding peak for RARA and RXRA in the first intron of *Halr1* in ESCs (at day 1 of differentiation) and a significant peak at the *Hoxa1* 3'-end (Figure 1E and F) (17,51), suggesting possible regulation of *Hoxa1* and *Halr1* by RARA and RXRA. Next, we overexpressed RXRA and RARA in ESCs and performed qRT-PCR analysis for *Hoxa1* and *Halr1* transcripts (Supplementary Figure S3). At day 1 of RA differentiation, expression levels of both were significantly up-regulated in cells overexpressing RARA and RXRA compared to the control cells (Figure 1G). We also established RARA and RXRA single or double knockout lines using the CRISPR-Cas9 system and analyzed *Hoxa1* and *Halr1* transcript levels by qRT-PCR (Supplementary Figure S4). Relative to wild-type (WT) controls, RARA and RXRA deletion, either singly or double KOs, significantly suppressed *Hoxa1* and *Halr1* transcript levels at day one differentiation (Figure 1H). Taken together, these findings overall suggest that *Hoxa1* and *Halr1* may be direct target genes of RA signaling.

RAREs are required for RA signaling-induced *Hoxa1* and *Halr1* expression

Previous studies have shown that the regulation of target gene expression by RA is dependent on the *cis*-functional RARE at target gene loci (16,52). Several functional target genes exhibiting RARE elements have been identified, such as *Cyp26* (53), *Hoxb1* (54–58) and *Hoxa7* (59). We analyzed ChIP-seq data showing significant co-binding of RARA/RXRA at the *Hoxa1* and *Halr1* loci (Figure 2A). However, whether these RAREs at the *Halr1*-*Hoxa1* locus are functional is unclear. To assess their functionality, we examined the region of RARA/RXRA co-binding

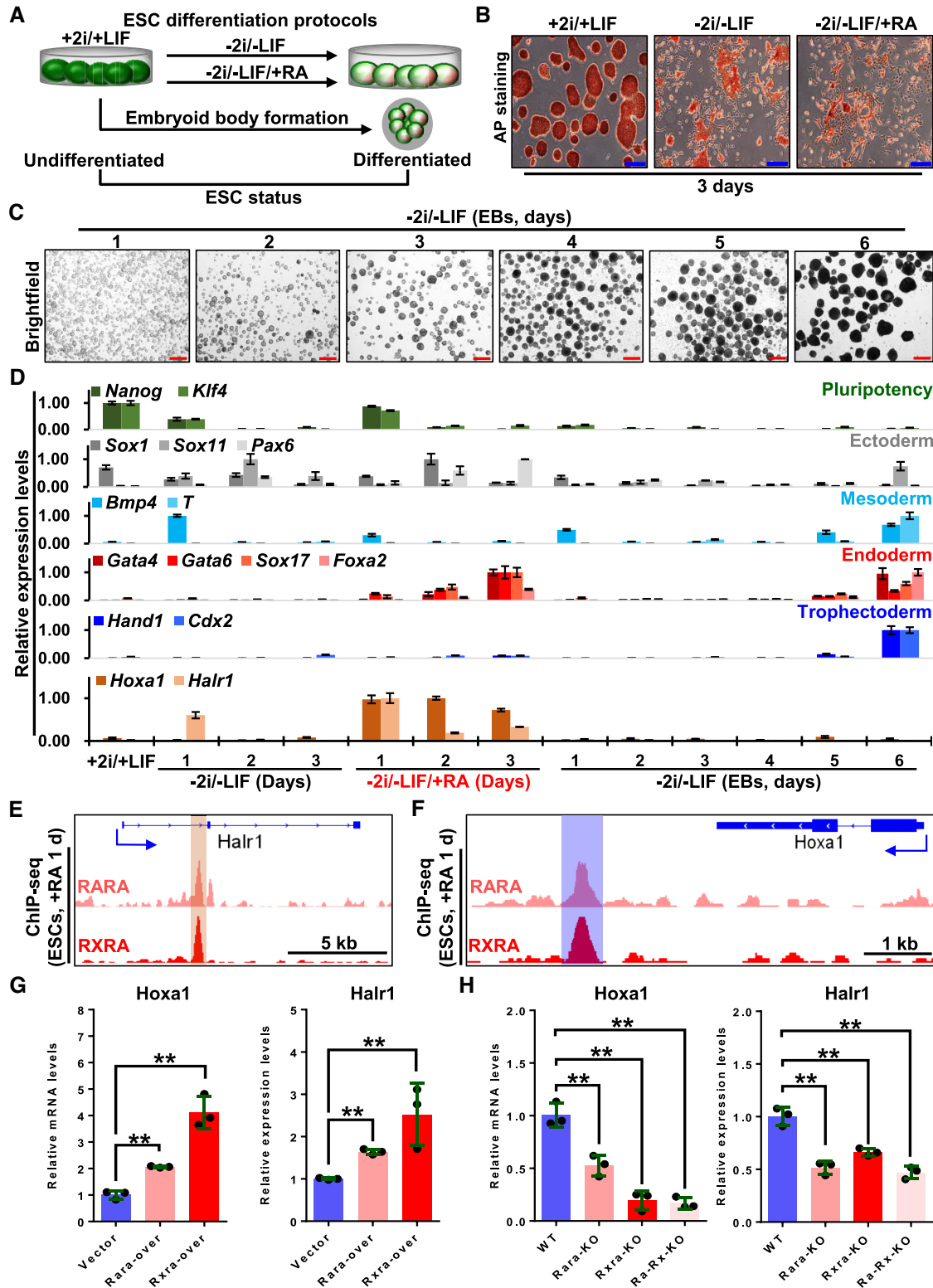


Figure 1. *Hoxa1* and *Halr1* are direct downstream target genes of RA signaling. (A) Schematic showing ESC differentiation protocols. (B) Images showing AP staining of undifferentiated and differentiated ESCs. Scale bars: 100 μ m. (C) Bright-field images of EBs on days 1–6. Scale bars: 200 μ m. (D) qRT-PCR data showing transcript levels of pluripotency and germ layer genes as well as *Halr1* and *Hoxa1* during ESC differentiation ($n = 3$ replicates). (E and F) ChIP-seq data showing RARA and RXRA binding peaks at *Halr1* and *Hoxa1* loci on day 1 of RA-induced ESC differentiation. (G) qRT-PCR data showing *Halr1* and *Hoxa1* transcript levels in ESCs overexpressing RARA and RXRA on day 1 of RA treatment. Data represent the mean \pm SD ($n = 3$ replicates). Statistical significance was determined by a two-tailed Student's *t*-test (unpaired), * $P < 0.05$, ** $P < 0.01$. (H) qRT-PCR data showing *Halr1* and *Hoxa1* transcript levels in WT or KO cells on day 1 of RA treatment. Data represent the mean \pm SD ($n = 3$ replicates). Statistical significance was determined by a two-tailed Student's *t*-test (unpaired), * $P < 0.05$, ** $P < 0.01$.

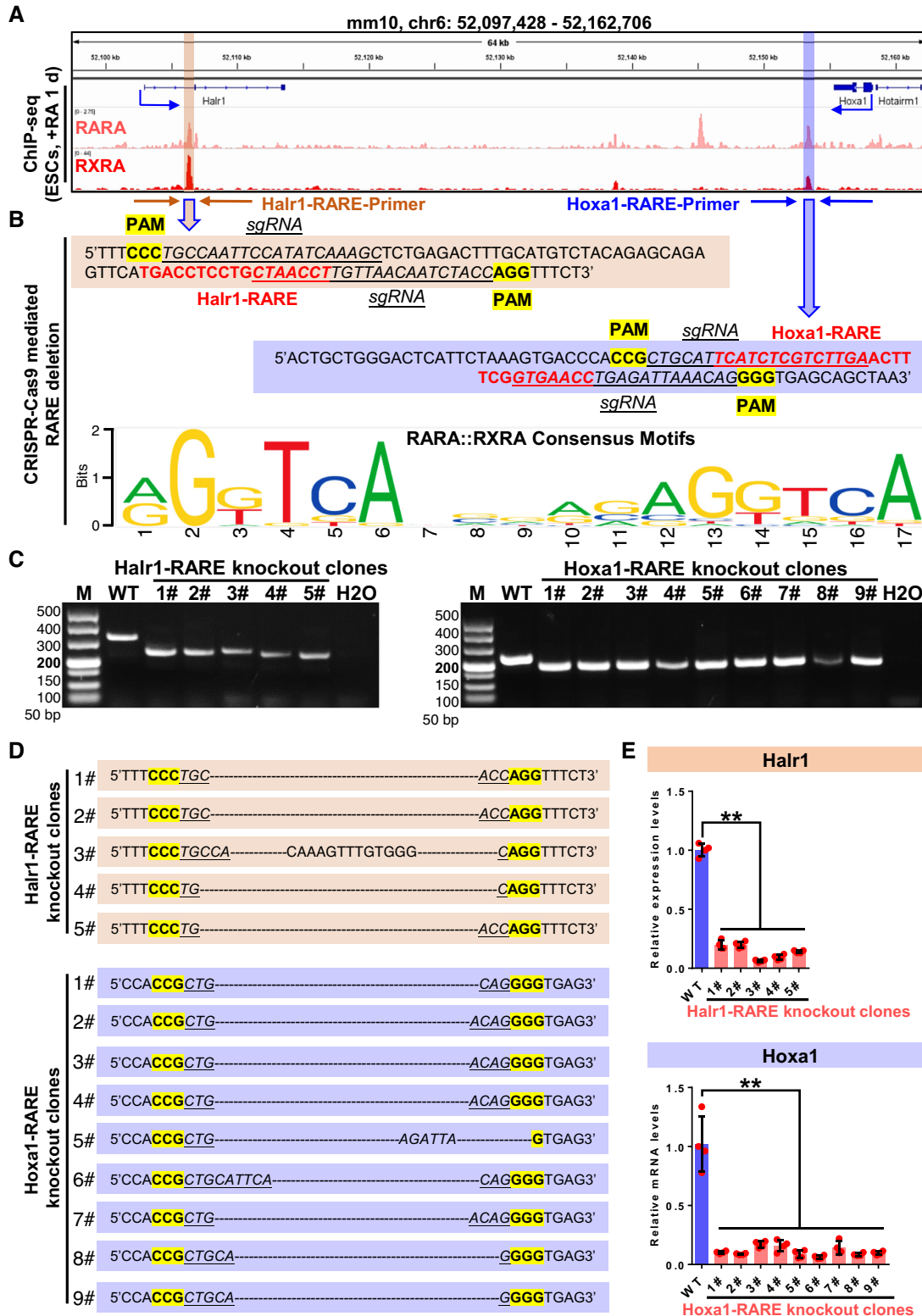


Figure 2. RAREs are required for RA signaling-induced *Hoxa1* and *Halr1* expression. (A) ChIP-seq data showing RARA and RXRA binding peaks at *Halr1* and *Hoxa1* loci in ESCs on day 1 of RA treatment. (B) JASPAR prediction of RAREs at the *Halr1*–*Hoxa1* locus, the RARA/RXRA binding structural domain, and the CRISPR-Cas9-mediated RARE knockout scheme. (C) Agarose gel electrophoresis showing RARE knockout clones using primers shown in (B). (D) Sanger sequencing of PCR products in (C). (E) qRT-PCR showing *Halr1* and *Hoxa1* transcript levels in RARE knockout cells. Data represent the mean ± SD ($n = 4$ replicates). Statistical significance was determined by a two-tailed Student's *t*-test (unpaired), * $P < 0.05$, ** $P < 0.01$. M: DNA ladder marker.

at these loci using the JASPAR database (60) and identified multiple putative RAREs (Figure 2B). We deleted these RAREs using the CRISPR–Cas9 system (Figure 2B) and then, using genomic-DNA PCR with specific primers and Sanger sequencing, we obtained multiple RARE knockout clones (Figure 2C and D; Supplementary Figure S5). RA treatment of RARE knockout cells resulted in significantly lower *Halr1* and *Hoxa1* transcript levels relative to WT cells (Figure 2E), strongly suggesting that these RAREs act as *cis*-functional elements necessary for RA signaling-dependent activation of *Hoxa1* and *Halr1* expression. Taken together, these results indicated that *Halr1* and *Hoxa1* are direct downstream targets of RA signaling and regulated by RARA/RXRA *via* RAREs.

Increased enhancer interactions promote RA signaling-induced *Hoxa1* and *Halr1* activation

Our previous study reported that there are three enhancers at the *Halr1–Hoxa1* locus, and in the RA-induced ESC differentiation state, the three enhancers significantly interact with each other to form an enhancer–enhancer interaction complex (EEIC) that regulates RA signaling-induced *HoxA* cluster gene expression (23). However, the pattern of interactions between these enhancers in the RA signaling-induced differentiated and undifferentiated states of ESCs and the regulation of *Hoxa1* and *Halr1* are unclear.

To investigate the chromatin interaction patterns of these enhancers during RA-induced early ESC differentiation, we used the Capture-C method (23,35,36,61), a 3C-based chromosome conformation capture technique (62). The three enhancers at the *Halr1–Hoxa1* locus served as anchor regions to perform enhancer capture using the capture-C method in undifferentiated and RA-induced differentiated ESCs (at day one) (Figure 3A and B) (28,63). Chromatin interactions between En1 and En2 under RA-induced ESC differentiation significantly increased, while En3 also showed significantly enhanced interactions with En1, En2 and *Hoxa1* chromatin, but reduced interactions with *HoxA* cluster chromatin (Figure 3C–E). These data suggest that a tight EEIC forms between enhancers during RA-induced early ESC differentiation and that these interactions with the *HoxA* cluster chromatin are also significantly enhanced. Considering previous results showing that RA signaling induces significant activation of *Hoxa1* and *Halr1* (Figure 1D), we hypothesize that there may be a positive correlation between increased enhancer interactions and high expression of *Hoxa1* and *Halr1*. To test the hypothesis, we treated both WT and enhancer KO cells with RA for one day and monitored *Hoxa1* and *Halr1* transcript levels by qRT-PCR (23). WT cells showed significant upregulation of *Hoxa1* and *Halr1* expression after RA treatment, relative to undifferentiated ESCs; however, RA-treated enhancer KO cells showed significantly reduced *Hoxa1* and *Halr1* expression (Figure 3F and G). In addition, Enhancer KO cells also showed significant suppression of other genes in the *HoxA* cluster (*Hoxa2–13*) (Supplementary Figure S6). Taken together, these data confirm the increase in enhancer interactions following stimulation of RA signaling at the *Halr1–Hoxa1* locus, further suggesting that these enhancers are required for the activation of *Hoxa1* and *Halr1*.

Enhancers are required for RA signaling-induced early proper lineage differentiation of ESCs

To further investigate whether these enhancers regulate RA signaling-induced early lineage differentiation of ESCs, we next performed RNA-seq analysis in WT and enhancer knockout cells after one day of RA treatment. Enhancer deletion resulted in significant changes in gene expression relative to WT cells (Supplementary Figure S7A). GO analysis of significantly altered gene groups (FD ≥ 2 , FDR < 0.05) revealed that tissue morphogenesis, heart development, embryonic organ development and other developmentally-related biological processes were significantly enriched in enhancer KO cells (Supplementary Figure S7B). Moreover, among specific genes related to ESC differentiation, *Bmp4*, *Gata3*, *Gata4*, *Wnt3a* and *Notch1* were enriched (Supplementary Figure S7C; Supplementary Table S8). These results suggest that enhancer deletion regulates RA signaling induced-early differentiation of ESCs.

Next, we also analyzed the changes in *Halr1* and *HoxA* cluster gene expression in RNA-seq data and found that enhancer deletions significantly suppressed *Halr1* and *HoxA* cluster gene expression (Figure 4A), a finding consistent with the qRT-PCR results. Furthermore, analysis of the expression of pluripotency and germ layer genes showed that enhancers' deletion significantly promotes the expression of pluripotency genes compared to WT cells, whereas the mesendoderm genes were significantly repressed, indicating that enhancers deletion inhibited RA-induced early mesendoderm differentiation of ESCs (Figure 4B and C). Cluster analysis of differentially-expressed genes and subsequent GO analysis revealed that multiple biological processes associated with differentiation were significantly enriched in enhancer deletion cells (Figure 4D and E; Supplementary Table S9), such as embryonic organ development, nervous system development, heart development and tissue morphogenesis. Taken together, these data suggest that in ESCs, these enhancers are required for induction of proper lineage differentiation by RA signaling.

HOXA1 promotes expression of *Halr1* through binding to enhancer

Previous studies have shown that HOXA1 plays an essential regulatory role as TF during RA signaling-induced early ESC differentiation (18,19,21). However, whether HOXA1 regulates lncRNA is unknown. Interestingly, by analyzing HOXA1 ChIP-seq data, we found significant binding of HOXA1 at the *Halr1* locus, and further analysis in conjunction with H3K27ac ChIP-seq data revealed significant co-localization of HOXA1 binding with enhancers at the *Halr1–Hoxa1* locus (Figure 5A) (21,28). These findings suggest that HOXA1 may be involved in regulating *Halr1* expression.

To determine whether HOXA1 regulates *Halr1* expression, we examined potential direct regulatory effects of HOXA1 on the *Halr1* gene using overexpression and loss-of-function studies. First, we overexpressed HOXA1 in undifferentiated ESCs and found significant differences in ESCs' cell morphology (Figure 5B–D). Further pluripotency gene assays revealed significant downregulation of *Nanog* and *Klf4*, while differentiation genes such as *Sox1*

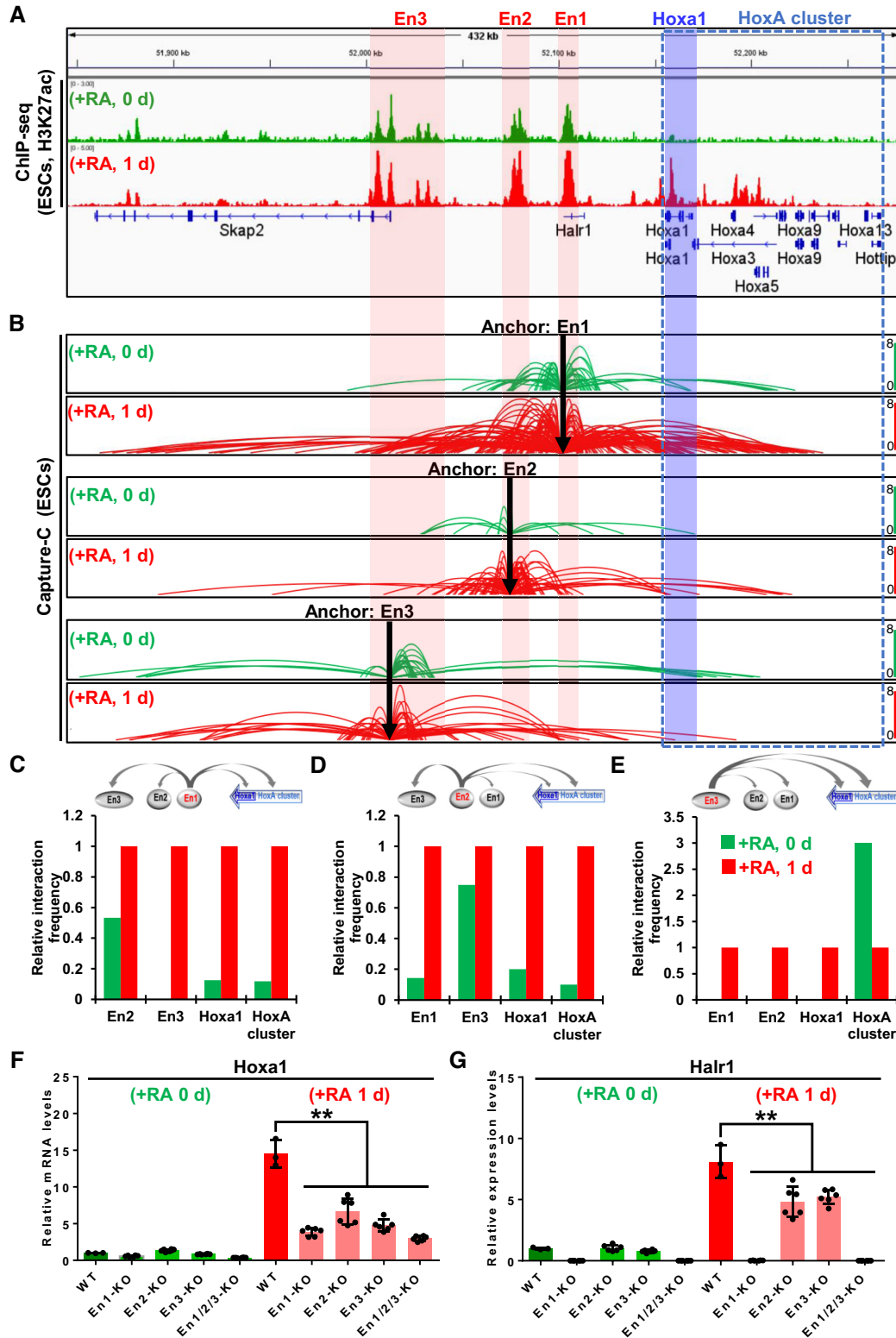


Figure 3. Increased enhancer interactions promote RA signaling-induced *Hoxa1* and *Halr1* activation. (A) H3K27ac ChIP-seq data in ESCs either untreated or treated 1 day with RA demonstrating enhancers at the *Halr1-Hoxa1* locus. (B) Chromatin loops showing enhancer Capture-C data over the course of RA-induced ESC differentiation. (C–E) Relative quantitative results showing enhancer interactions during RA-induced ESC differentiation. (F, G) qRT-PCR results showing *Halr1* and *Hoxa1* transcript levels after enhancer KO during RA-induced ESC differentiation. Data represent the mean \pm SD, $n = 3$ or 6 replicates for WT or enhancer knockout cells. Statistical significance was determined by a two-tailed Student's *t*-test (unpaired), * $P < 0.05$, ** $P < 0.01$.

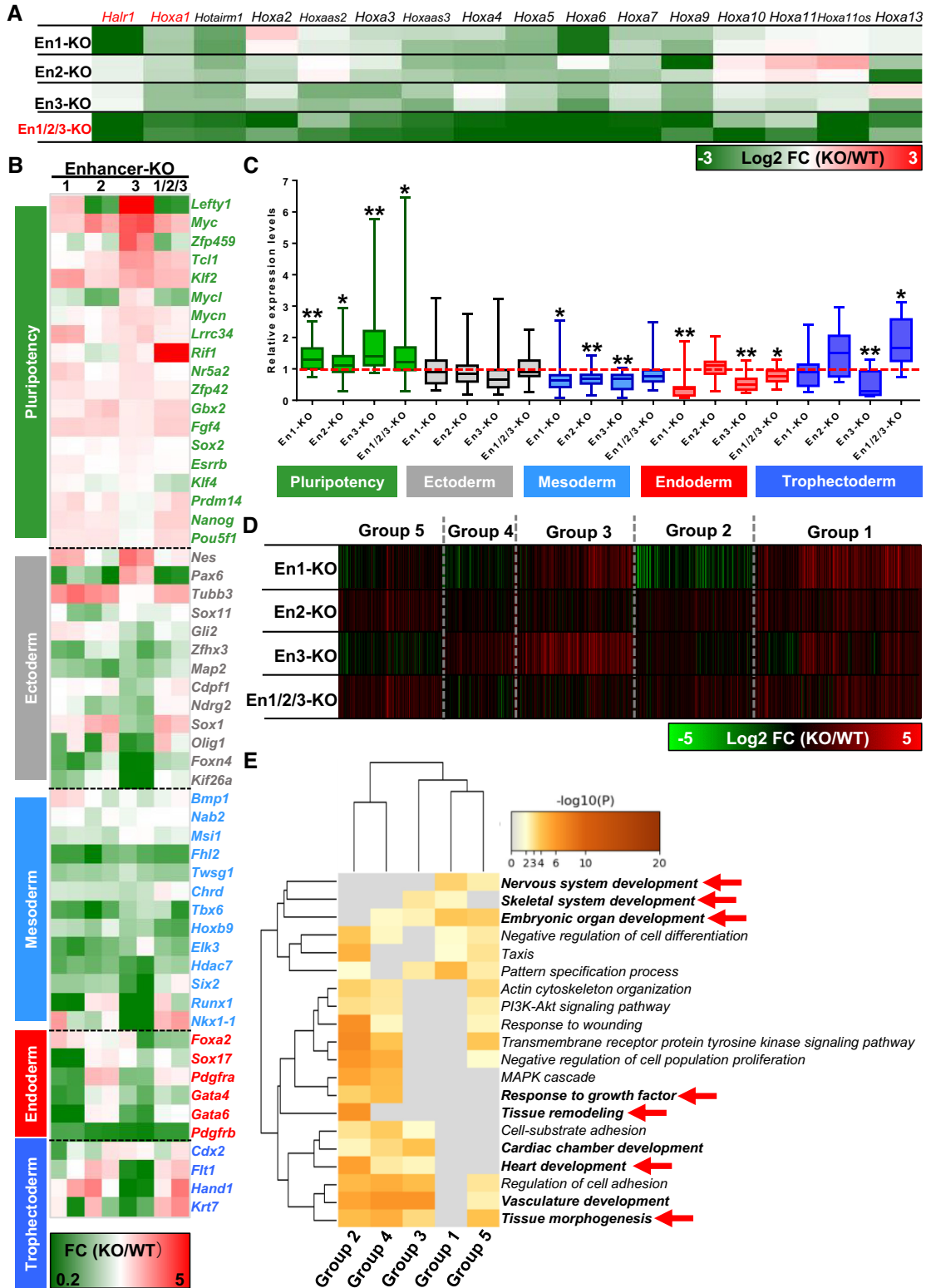


Figure 4. Enhancers are required for RA signaling-induced early proper lineage differentiation of ESCs. (A) Heatmap showing relative transcript levels of *Halr1* and *HoxA* cluster genes in enhancer KO ESCs at day 1 of RA treatment. (B) Heatmap showing relative transcript levels of pluripotency and germ layer genes in enhancer KO cells at day 1 of RA treatment. (C) Results showing changes in expression of pluripotency or germ layer genes in enhancer KO relative to WT ESCs (RNA-seq data). Expression levels in WT ESCs were set to 1 and shown as the red dotted line. (D) Cluster analysis of differentially-expressed genes in enhancer KO cells. (E) GO-BP analysis of gene clusters obtained in (D).

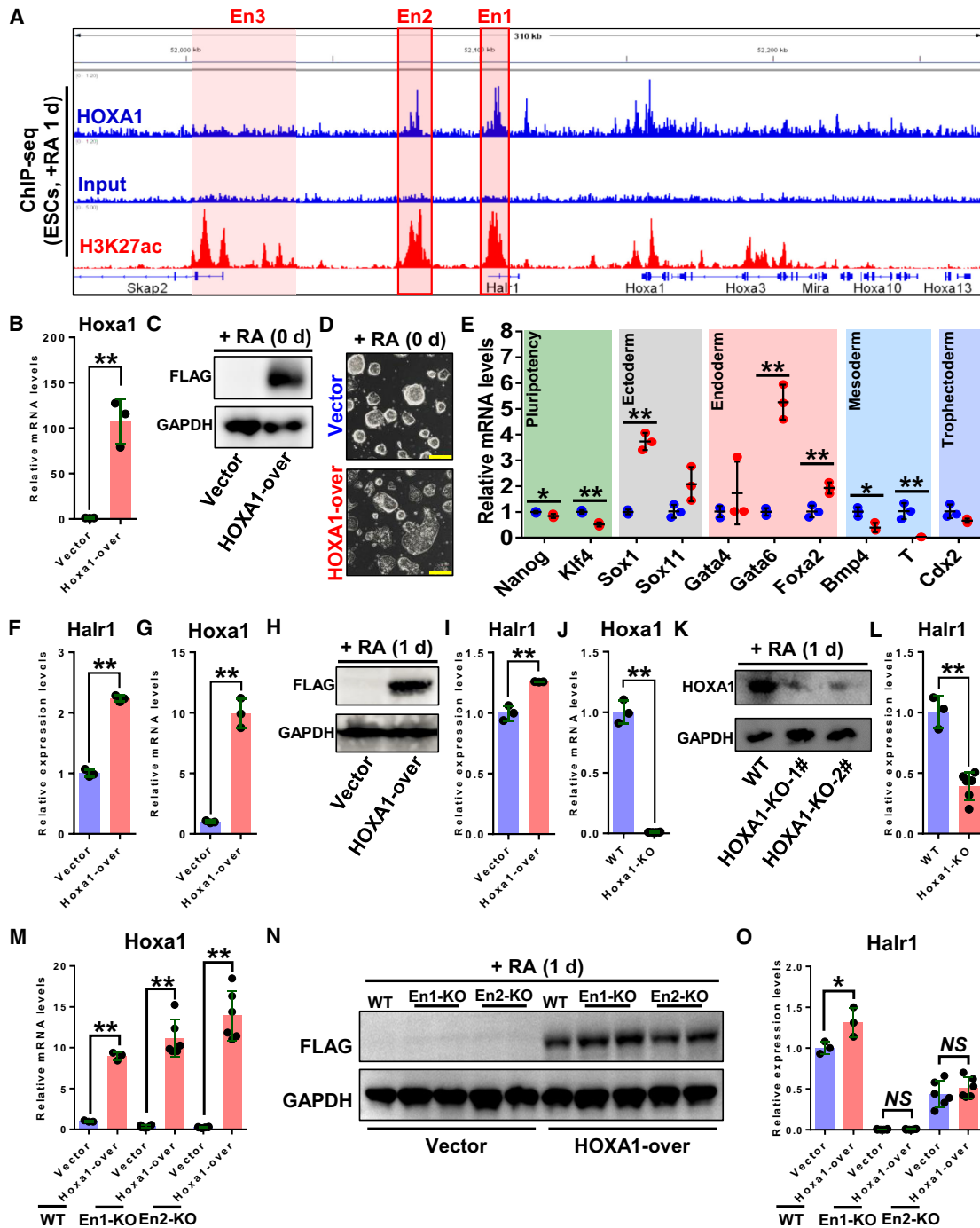


Figure 5. HOXA1 promotes *Halr1* expression through binding to enhancers. (A) Enrichment of HOXA1 and H3K27ac ChIP-seq signals at the *Halr1*-*Hoxa1* locus. (B) qRT-PCR analysis of *Hoxa1* transcript levels in ESCs transfected with vector control or HOXA1 overexpression plasmids. (C) WB analysis of HOXA1 protein levels in ESCs transfected as in (B). (D) Bright-field images showing ESC morphology after HOXA1 overexpression. Scale bars: 100 μ m. (E) qRT-PCR analysis of pluripotency and germ layer transcripts in ESCs transfected with control vector or HOXA1 overexpression plasmids. (F) qRT-PCR analysis of *Halr1* transcript levels in ESCs transfected with vector control or HOXA1 overexpression plasmids. (G) qRT-PCR analysis of *Hoxa1* mRNA levels in ESCs transfected with control vector or HOXA1 overexpression plasmids on day 1 of RA treatment. (H) WB analysis of HOXA1 protein levels in cells transfected as in (G). (I) qRT-PCR analysis of *Halr1* RNA expression levels in ESCs transfected with control vector or HOXA1 overexpression plasmids on day 1 of RA treatment. (J) qRT-PCR analysis of *Hoxa1* transcript levels in WT and *Hoxa1* KO cells on day 1 of RA treatment. (K) WB analysis of HOXA1 protein levels in cells transfected as in (J). (L) qRT-PCR analysis of *Halr1* transcript levels in WT and *Hoxa1* KO cells on day 1 of RA treatment. (M) qRT-PCR analysis of *Hoxa1* transcript levels in WT and enhancer KO cells transfected with control vector or HOXA1 overexpression plasmids on day 1 of RA treatment. (N) WB analysis of HOXA1 protein levels in cells transfected as in (M). (O) qRT-PCR analysis of *Halr1* transcript levels in WT and enhancer KO cells transfected with control vector or HOXA1 overexpression plasmids on day 1 of RA treatment. NS: not significant. In (B), (E–G), (I), (J), (L), (M) and (O), data represent the mean \pm SD ($n = 3$ or 6 replicates). Statistical significance was determined by a two-tailed Student's *t*-test (unpaired), * $P < 0.05$, ** $P < 0.01$.

(ectoderm), *Gata6* and *Foxa2* (endoderm) were significantly upregulated and mesoderm genes (*Bmp4* and *T*) were significantly downregulated in HOXA1-over ESC, suggesting that HOXA1 overexpression perturbs ESC pluripotency (Figure 5E). qRT-PCR analysis of ESCs overexpressing HOXA1 showed significantly higher *Halr1* expression compared with vector control, suggesting that HOXA1 promotes *Halr1* expression in ESCs (Figure 5F). Following RA-induced ESC differentiation, HOXA1 overexpression still upregulated *Halr1* expression (Figure 5G–I). Further, we used CRISPR-Cas9 technology to knockout HOXA1 and assess effects on *Halr1* expression (Supplementary Figure S8). qRT-PCR analysis showed significantly decreased *Halr1* transcript levels in HOXA1 KO ESCs after RA treatment compared to comparably treated WT cells (Figure 5J–L). This combined with the HOXA1 ChIP-seq data suggests that HOXA1 directly regulates *Halr1* expression.

Considering the significant binding of HOXA1 to enhancer En1 and En2 (Figure 5A), we asked whether the promoting effect of HOXA1 on *Halr1* expression was enhancer-dependent. To do so, we overexpressed HOXA1 in WT and in En1 or En2 enhancer KO cells (Figure 5M and N). After 1 day of RA treatment, WT cells overexpressing HOXA1 showed increased *Halr1* expression, while enhancers (En1 and En2) knockout cells overexpressing HOXA1 showed no change in *Halr1* expression (Figure 5O). These results suggest that enhancers are required for HOXA1 to promote *Halr1* expression during RA-induced early differentiation of ESCs. Further, to assess direct regulatory effects, we also knockout the HOXA1 binding sites (H1BSs) at these enhancer regions (En1 and En2) by using CRISPR-Cas9 technology (Supplementary Figure S9A–D). qRT-PCR results showed that deletion of these H1BSs significantly suppressed RA-induced *Halr1* expression, indicating the direct regulatory effect of HOXA1 on *Halr1* (Supplementary Figure S9E). Taken together, these data suggest that HOXA1 promotes *Halr1* expression through these enhancers.

***Halr1* orchestrates the *Hoxal* chromatin structure by acting as the ‘brake’ and the ‘binder’**

Previous studies have shown that long noncoding RNAs regulate gene expression through multiple modes, such as acting as sponges for microRNAs or as scaffolds that interact with proteins to regulate target gene expression (64–66). *Halr1* transcription site has significant H3K27ac labeling and knockout of enhancer En1 abolishes *Halr1* expression, suggesting that *Halr1* may be an enhancer-associated RNA (eRNA) (Figure 6A).

A recent study showed that *Halr1* RNA regulates *HoxA* cluster expression mainly by binding *HoxA* cluster chromatin (27). Our analysis of *Halr1* ChIRP-DNA-seq data (27), combined with Hi-C data (8,47), revealed that *Halr1* is mainly enriched at the *Halr1-Hoxal* locus and is located within the same topologically associating domain (TAD) (Figure 6B; Supplementary Figure S10). To determine if *Halr1* regulates *Hoxal* chromatin structure, we again used Capture-C technology to compare chromatin interactions in WT and *Halr1*-KO cells using the *Hoxal* locus as the anchor region (Figure 6C). *Halr1* deletion significantly al-

tered *Hoxal* chromatin interactions, and in *Halr1*-KO cells, *Hoxal* chromatin interactions with enhancers En1 and En2 significantly increased, while interactions with enhancer En3 and *HoxA* cluster chromatin decreased (Figure 6D). In addition, we also unexpectedly observed increased interactions of two distal mini-enhancers (mEn1 and mEn2) with *Hoxal* chromatin in *Halr1*-KO cells (Figure 6C). These results suggest that *Halr1* RNA bound to chromatin acts as a scaffold, on one hand, as a ‘binder’ to facilitate interaction of *Hoxal* chromatin with enhancer En3 and maintain the *HoxA* cluster chromatin structure, and on the other hand, as a ‘brake’ to inhibit interaction of *Hoxal* chromatin with enhancers En1 and En2 and two distal mini-enhancers (mEn1 and mEn2).

***Halr1* deletion promotes RA signaling-induced *Hoxal* over-activation and early endoderm differentiation of ESCs**

To investigate the regulation of *Hoxal* expression by *Halr1*, we examined the mRNA expression levels of *Hoxal* by qRT-PCR and showed that the mRNA expression levels of *Hoxal* were significantly increased in *Halr1*-KO cells when compared with WT cells in the presence of RA treatment (Figure 6E). In addition, expression of other *HoxA* cluster genes (*Hoxa2–13*) was also significantly increased in *Halr1*-KO cells, consistent with previous reports (27,29). Considering that deletion of *Halr1* also increases the interaction of *Hoxal* with two distal mini-enhancers (mEn1 and mEn2), it is unclear whether these enhancers regulate RA signaling-induced *Hoxal* expression. Next, we also generated the two distal mini-enhancers knockout cells by using CRISPR-Cas9 technology (Supplementary Figure S11). At day one after RA treatment, qRT-PCR analysis indicated significant decreased *Hoxal* transcript levels relative to comparably treated WT cells (Figure 6F), indicating that the two distal mini-enhancers are also required for RA-induced *Hoxal* expression and are newly identified *Hoxal* enhancers. Taken together, these data suggest that *Halr1* plays a critical role in suppressing *Hoxal* expression during RA-induced early differentiation of ESCs.

To further investigate the regulatory effect of *Halr1* in the early stages of RA-induced ESC differentiation, we performed RNA-seq in WT and *Halr1*-KO cells at day one after RA treatment. *Halr1* deletion significantly altered gene expression (Figure 7A; Supplementary Figure S12A), and *HoxA* cluster genes were significantly up-regulated (Figure 7B), consistent with qRT-PCR results (Figure 6E). Further analysis of pluripotency and germ layer genes revealed that pluripotency and ectodermal genes were significantly down-regulated, while meso-endoderm was significantly up-regulated, especially endoderm genes were more significantly up-regulated (Figure 7C and D). Further GO-BP analysis revealed that up-regulated genes were significantly enriched in biological processes related to embryonic skeletal system morphogenesis, endoderm formation and endodermal cell differentiation, while down-regulated genes were significantly enriched in processes associated with stem cell population maintenance (Figure 7E; Supplementary Table S10). GSEA of these biological processes also showed significant differences (Figure 7F and G). In summary, these results suggest that *Halr1* is required for

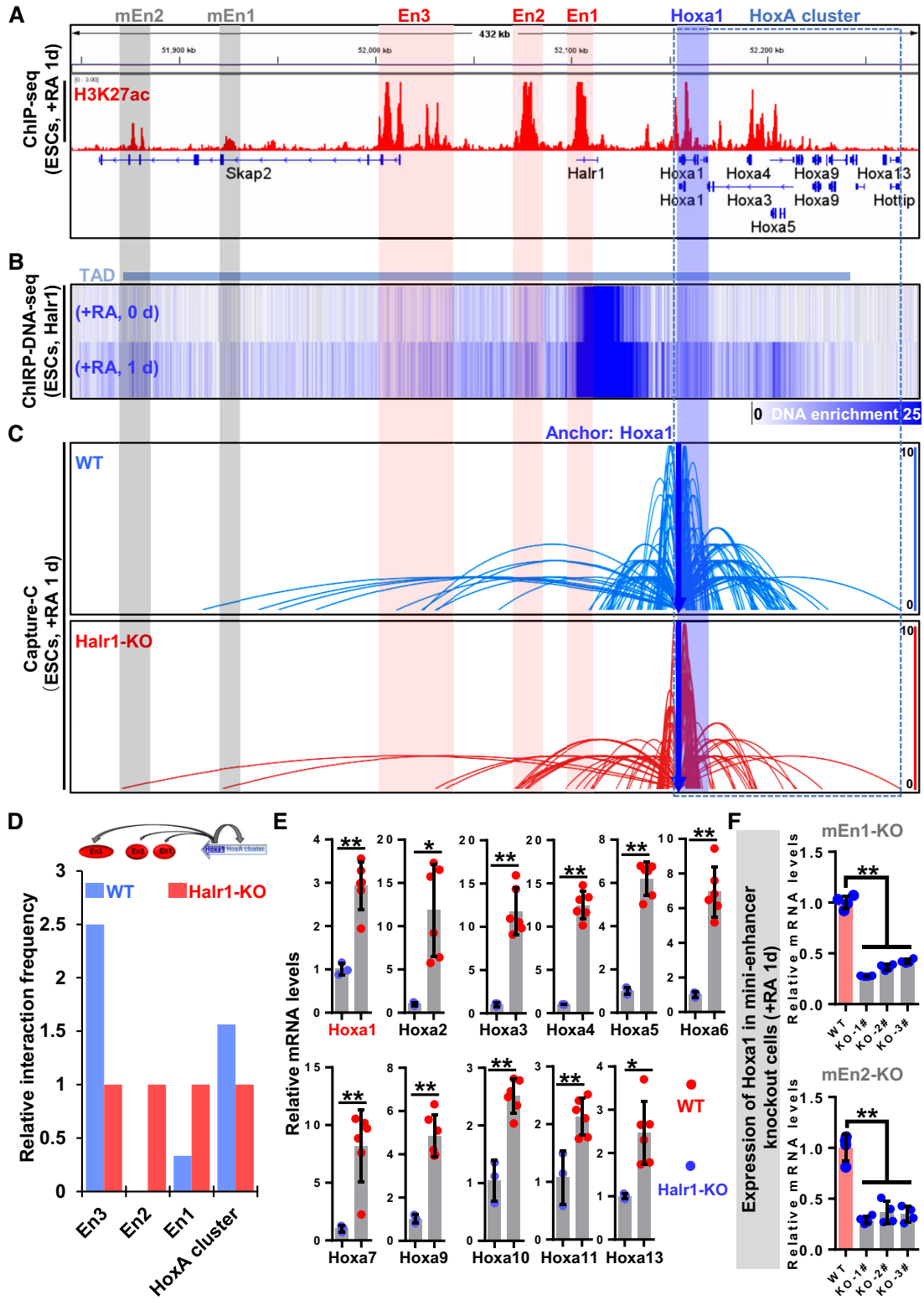


Figure 6. *Halr1* RNA orchestrates *Hoxal* chromatin interactions during RA signaling-induced early differentiation of ESCs. (A) ChIP-seq data demonstrating H3K27ac enrichment at the *Halr1-Hoxa1* locus. (B) ChIRP-seq data demonstrating *Halr1* RNA enrichment at the *Halr1-Hoxal* locus. (C) Chromatin loops showing *Hoxal* Capture-C data demonstrating *Hoxal* chromatin interactions after *Halr1* deletion. (D) Relative quantitative results demonstrating changes in *Hoxal* chromatin interactions after *Halr1* deletion. (E) Heatmap showing transcript levels of *HoxA* cluster genes in WT and *Halr1*-KO ESCs on day 1 of RA treatment. (F) Expression levels of *Hoxal* mRNAs in mini-enhancer knockout cells. Data represent the mean \pm SD ($n = 4$ replicates). Statistical significance was determined by a two-tailed Student's *t*-test (unpaired), * $P < 0.05$, ** $P < 0.01$.

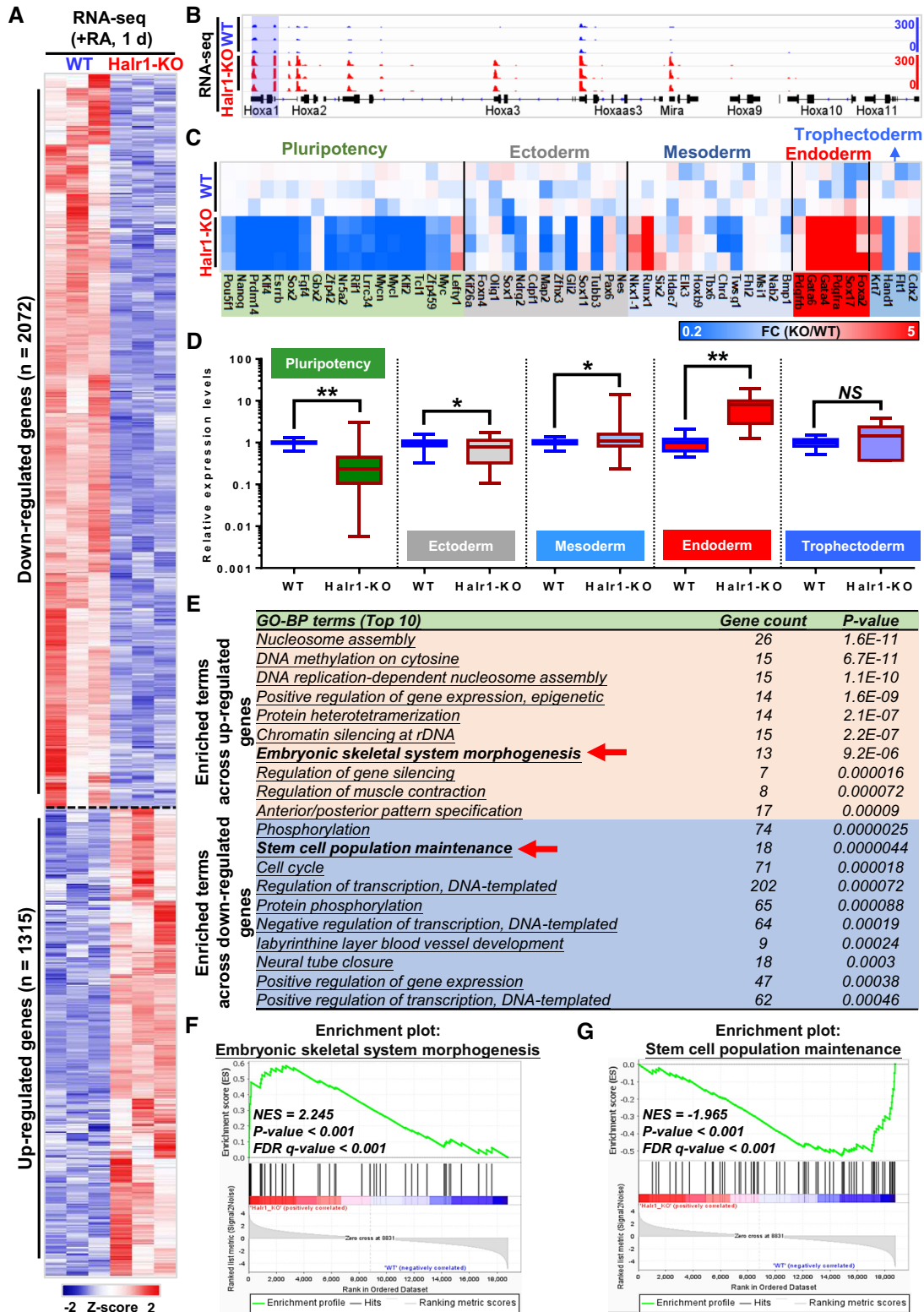


Figure 7. *Hafr1* deletion promotes RA signaling-induced *Hoxa1* overactivation and enhanced early endodermal differentiation of ESCs. (A) Heatmap showing genes differentially-expressed in WT and *Hafr1*-KO cells. (B) IGV screenshots showing *HoxA* cluster gene expression levels in WT and *Hafr1*-KO cells. (C) Heatmap showing expression levels of pluripotency and germ layer genes in WT and *Hafr1*-KO cells. (D) Results showing changes in pluripotency and germ layer gene expression in *Hafr1*-KO relative to WT cells (RNA-seq data). (E) GO analysis showing biological processes of differential gene enrichment (Top 10). (F, G) Gene Set Enrichment Analysis (GSEA) of genes differentially expressed in *Hafr1*-KO versus WT ESCs among genes associated with embryonic skeletal system morphogenesis (F) and stem cell population maintenance (G).

RA signaling-induced early proper differentiation of ESCs, particularly of the endoderm.

***Hoxa1* cooperates with *Halr1* to regulate RA signaling-induced early lineage differentiation of ESCs**

Our findings suggest that RA signaling activates *Hoxa1* and *Halr1* expression, and concomitantly, HOXA1 promotes *Halr1* expression, which in turn represses *Hoxa1* expression. Given these complex relationships, we established *Hoxa1/Halr1* double-knockout (DKO) lines to investigate effects on RA signaling-induced early ESC differentiation (Supplementary Figure S8). RNA-seq data revealed that *Hoxa1/Halr1* DKO significantly altered gene expression (Supplementary Figure S12A), and GO analysis of genes differentially expressed in single or double knockout cells revealed significant enrichment for biological processes associated with ESC development, such as heart development, tissue morphogenesis, gliogenesis, embryonic morphogenesis and cell fate commitment (Supplementary Figure S12B). Further analysis of biological processes associated with endoderm revealed changes in expression of several TFs significantly associated with endoderm development, such as *Sox9*, *Gata3*, *Gata4* and *Gata6* (Supplementary Figure S12C; Supplementary Table S11).

To reveal the co-regulatory effects of *Hoxa1* and *Halr1* in RA signaling-induced early lineage differentiation of ESCs, we also analyzed pluripotency and germ layer genes expression in these knockout cells (Figure 8A). Among them, *Halr1* KO promoted endoderm gene expression relative to WT cells, while *Hoxa1* KO suppressed endoderm gene expression, whereas endoderm gene expression in DKO cells did not differ significantly (Figure 8B). These results reveal that RA signaling-induced early proper lineage differentiation of ESC requires expressions of *Hoxa1* and *Halr1*. Further, GO analysis after combining these differential genes in knockout cells revealed significant enrichment in biological processes related to heart development, vasculature development, nervous system development and embryonic morphogenesis (Figure 8C and D; Supplementary Table S12). Taken together, these results suggest that *Hoxa1* and *Halr1* co-expression maintains RA signaling-induced early ESC proper lineage differentiation.

HOXA1 acts as a core transcriptional regulator and directly regulates the expression of a subset of genes associated with endoderm development

Considering that both enhancers and *Halr1* can regulate *Hoxa1* expression, and HOXA1, as a transcription factor, has extensive downstream regulation within the genome (18,21). To further characterize the regulatory effects of enhancers and *Halr1* through HOXA1 during RA-induced early ESC differentiation. We also analyzed the distribution of HOXA1 binding within the genome (Figure 9A), and HOXA1-bound genes were analyzed together with differential genes in various knockout cells using RNA-seq data. That analysis resulted in seven gene sets (Figure 9B). Subsequent GO analysis revealed significant enrichment in biological processes such as stem cell differentiation, developmental growth involved in morphogenesis, and embryonic morphogenesis (Figure 9C), suggesting that HOXA1

may be directly involved in RA-induced ESC differentiation as an executor in these regulatory processes. Furthermore, to identify gene sets related to endoderm development, we selected five gene sets enriched in developmental processes and after overlap identified a cluster of genes directly regulated by HOXA1, including *Gata4*, *Wnt7b* and *Wnt3a* (Figure 9D and E; Supplementary Table S13).

DISCUSSION

Temporally and spatially precise transcription of genes is critical for ESC fate decisions. However, mechanisms underlying this process remain largely unclear. Previous studies have revealed that many TFs play a central role in controlling gene expression during ESC differentiation (2). However, recent studies of high-order chromatin structure and long non-coding RNAs have provided new insights into the precise intrinsic mechanisms underlying the regulation of gene expression (67–69). In this study, we report enhancer architecture-dependent multilayered transcriptional regulation at the *Halr1–Hoxa1* locus orchestrating RA signaling-induced early lineage differentiation of ESCs. Our results reveal a novel mechanism by which RA signaling facilitates correct ESC fate decisions during early differentiation via synergistic activity of enhancer elements, TFs and lncRNA (Figure 10).

Maintenance of ESC pluripotency requires activation of LIF signaling and inhibition of MEK and GSK3 pathways (70,71). When stimulation of these signaling pathways is withdrawn, the ESCs differentiate. In our random differentiation conditions lacking RA, ESCs show marked ectodermal differentiation with high expression of ectodermal master control TFs *Sox1* and *Sox11*. By contrast, RA-induced ESC differentiation also activated endodermal master control TFs such as *Gata4*, *Gata6*, *Sox17* and *Foxa2*, as well as ectodermal differentiation genes (Figure 1D), indicative of mixed lineage differentiation at this early point (Figure 10A). Indeed, it has also been previously reported that RA signaling significantly activates endoderm master control TFs during ESC differentiation, already suggesting RA-induced ESC endoderm differentiation (25,26). In addition, recent reports reveal that in ESCs, RA signaling significantly activates **2cell-like** (2C-like) marker expression, such as *Zscan4*, suggesting that RA also facilitates ESC conversion to a **2C-like cell state** (2CLC) (72–75). Interestingly, in our data (Supplementary Figure S13), we also found that the expression of *Zscan4* was significantly increased during RA-induced early ESC differentiation, while enhancers and *Hoxa1* both modulate *Zscan4* expressions. These findings suggest that RA signaling-induced early ESC lineage differentiation may be more complex, and molecular mechanisms underlying these complex activities warrant further analysis.

TF-driven transcription plays a central role in ESC differentiation (76,77). In our present study, the results reveal that early ESC differentiation after RA treatment is regulated on multiple levels (Figure 10B). First, we conclude that *Hoxa1* and *Halr1* are the direct downstream target genes of RA signaling regulated by RARA/RXRA via RAREs. The RARE at the 3'-end of *Hoxa1* was previously reported as required for RA-induced *Hoxa1* expression (78,79), and our results support this conclusion in our differentiation

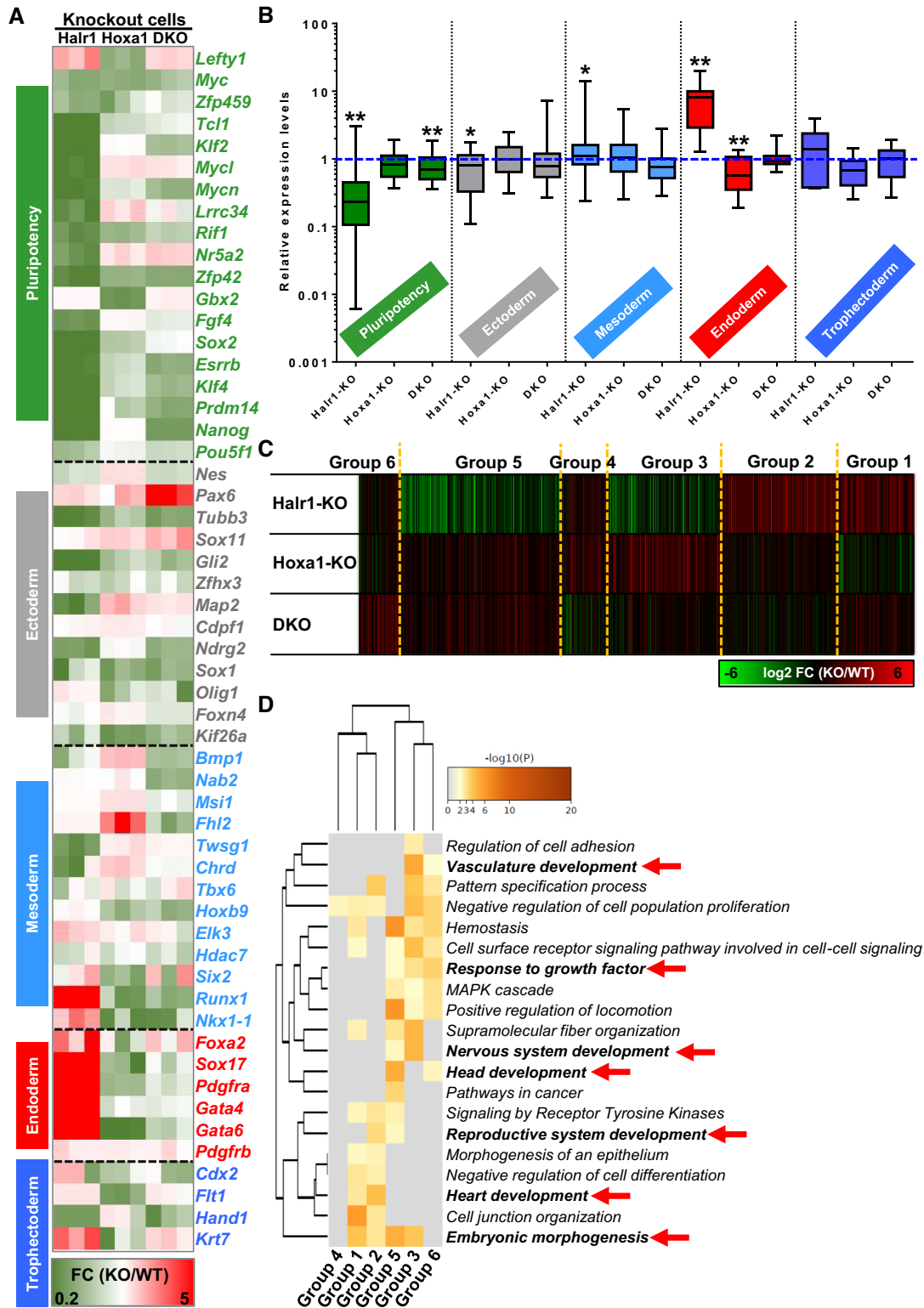


Figure 8. *Hoxa1* cooperates with *Halr1* to regulate RA signaling-induced early lineage differentiation of ESCs. (A) Heatmap showing expression of pluripotency and germ layer genes (RNA-seq data). (B) Changes in expression of pluripotency and germ layer genes in indicated single or double KO relative to WT cells (RNA-seq data). Expression levels in WT ESCs were set to 1 and shown as the blue dotted line. (C) Cluster analysis of genes differentially expressed in *Halr1*-KO, *Hoxa1*-KO and DKO cells. (D) GO-BP analysis of gene clusters obtained in (C).

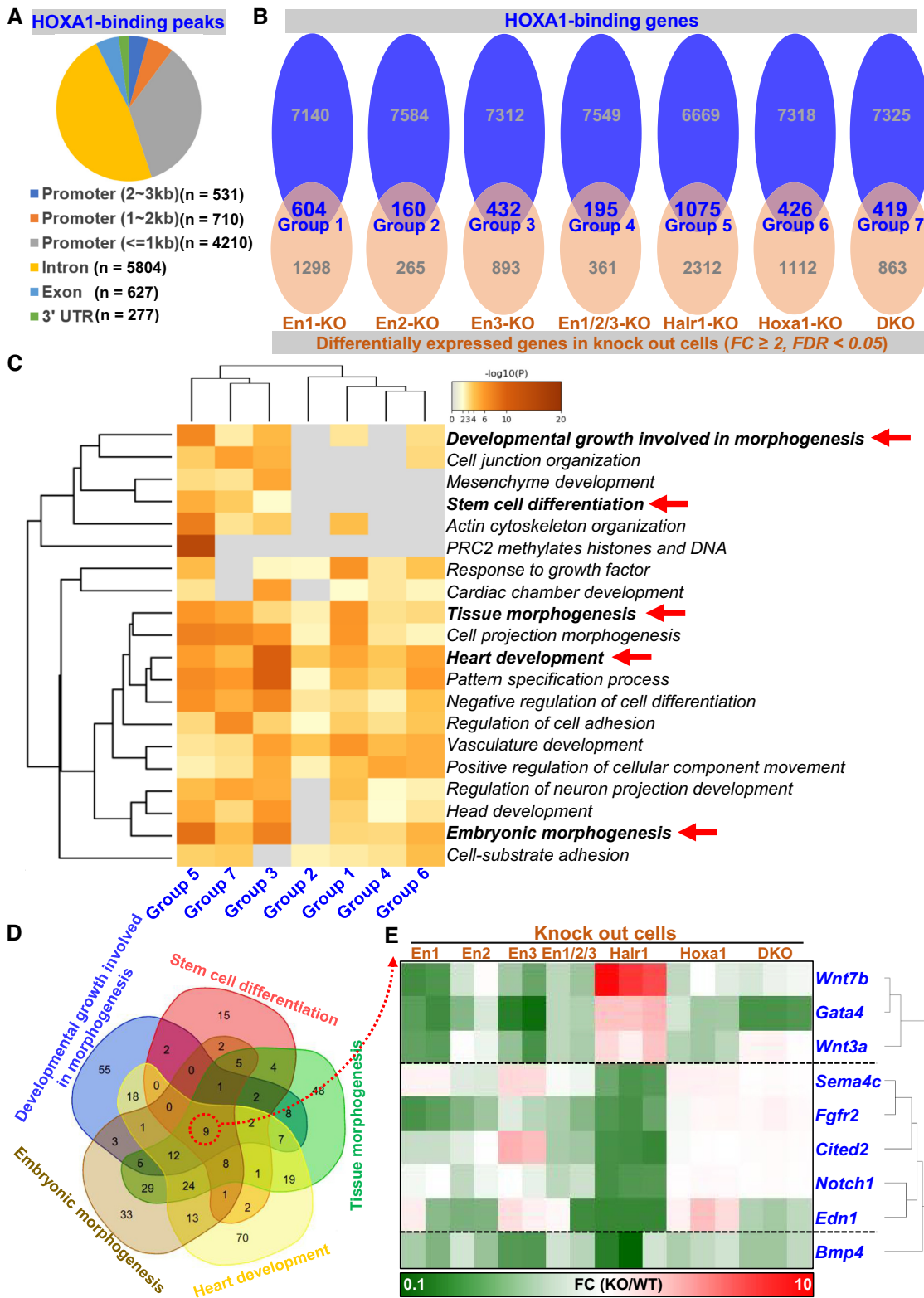


Figure 9. The core transcriptional regulator HOXA1 directly regulates expression of a subset of endodermal development-related genes. (A) Data showing the proportion of HOXA1 binding peaks in various genomic loci. (B) Comprehensive analysis of differential genes enriched for regulation by HOXA1. (C) GO-BP analysis of gene clusters obtained in (B). (D) Demonstration of common genes in selected biological process. (E) Heatmap showing expression levels of genes overlapped in (D).

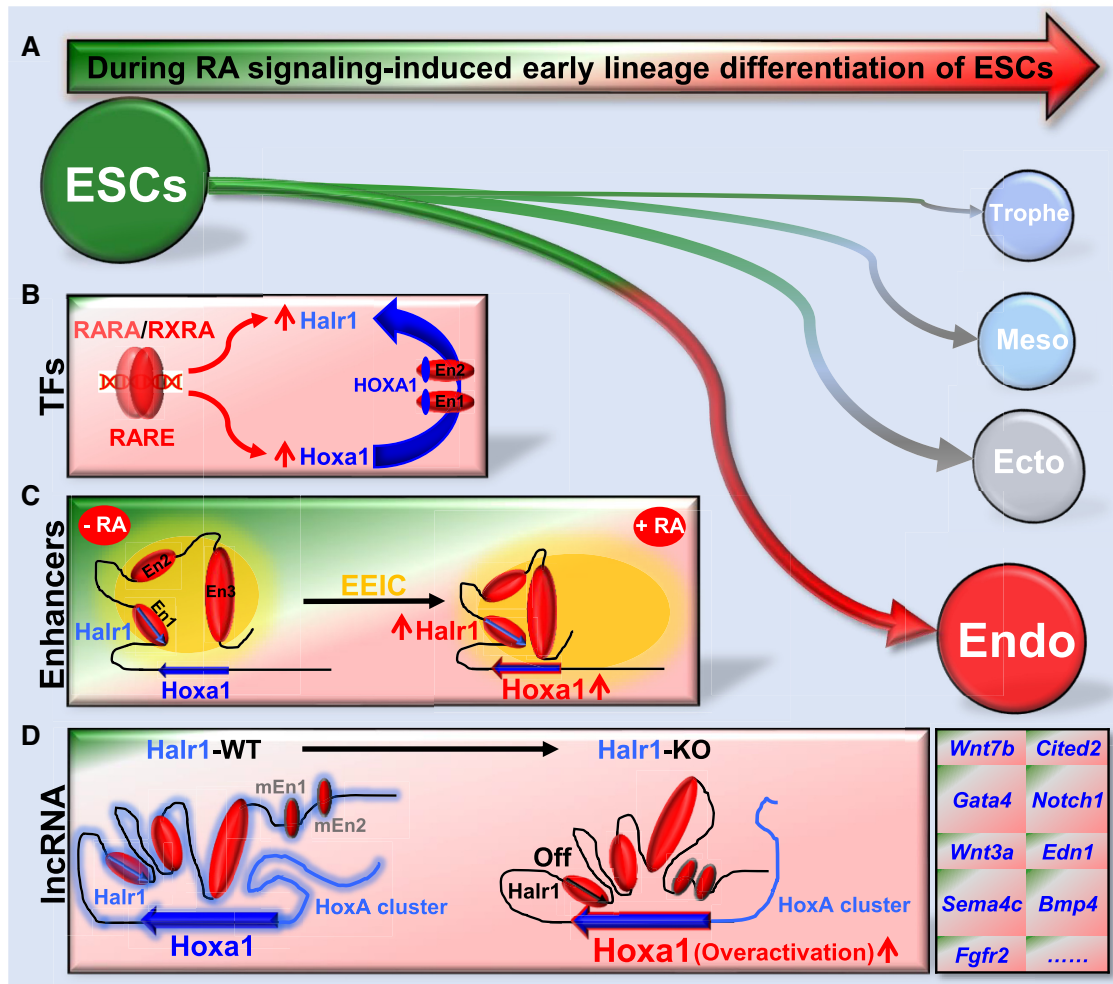


Figure 10. Schematic summary of this study. Schematic showing enhancer architecture-dependent multilayered transcriptional regulation at the *Halr1–Hoxa1* locus during RA signaling-induced early lineage differentiation of ESCs (A). (B) TF-driven gene expression: RARA/RXRA activates *Halr1* and *Hoxa1* expression via RAREs, and HOXA1 promotes *Halr1* expression through binding to enhancer regions. (C) Enhancer-dependent transcriptional regulation: RA promotes increased interactions between enhancers, resulting in a tighter EEIC and expression of *Halr1* and *Hoxa1*. (D) IncRNA *Halr1*-mediated chromatin organization orchestrates *Hoxa1* expression: *Halr1* RNA bound to DNA acts as a scaffold for chromatin structure, first as a binder to facilitate *Hoxa1* chromatin interaction with enhancer En3 and to maintain *HoxA* cluster chromatin structure, and second as a braking element to inhibit *Hoxa1* chromatin interaction with four distal enhancers (En1, En2 and mini-enhancers). Endo, endoderm; Ecto, ectoderm; Meso, mesoderm; Trophe, trophoderm.

model. However, a RARE within the *Halr1* locus has not until now been reported, and mechanisms underlying high expression of *Halr1* induced by RA signaling were not clear. Here, we identify a RARE within the *Halr1* locus that is functionally comparable to that of *Hoxa1* and required for RA signaling to promote high *Halr1* expression. Secondly, our results also further reveal that HOXA1 can directly promote *Halr1* expression. HOXA1 is a core TF in RA signaling-induced early ESC differentiation, and previous studies have primarily characterized its regulation of coding genes (18,21), but whether it can regulate the expression of long non-coding RNAs has not been reported. Here, we show that HOXA1 can regulate expression of the IncRNA *Halr1*, expanding its TF function. Thus, our study reveals a novel model of multilayered regulation driven by TFs during RA signaling-induced early ESC lineage differentiation, whereby RARA/RXRA activates the expression of

Hoxa1 and *Halr1*, while HOXA1 further promotes *Halr1* expression. Furthermore, considering that both RA receptors (RARA/RXRA) and HOXA1 bind and exert regulatory effects at the *Halr1–Hoxa1* locus during RA signaling-induced early ESC differentiation, the combined data above suggest that the regulation of RA signaling at the *Halr1–Hoxa1* locus is more likely to be the result of synergistic regulation by multi-factor, while the more refined underlying mechanisms may require further validation.

Enhancer is essential as the functional DNA element in ESCs maintenance and individual development (3). We previously showed that enhancer interactions during RA-induced ESC early differentiation result in formation of an EEIC that regulates *HoxA* cluster gene expression (23). In this study, we compared enhancer interactions in ESCs in both undifferentiated and RA-induced differentiation states and showed that RA signaling promoted enhancer

interactions, with some results similar to those previously reported (28), revealing dynamic chromatin interactions at the *Halr1-Hoxa1* locus (Figure 10C). Subsequently, our further analysis indicated that these enhancers are required for RA-induced *Hoxa1* and *Halr1* expression and early ESC lineage differentiation, particularly regulating mesendoderm differentiation, which has not been previously reported. We recently reported that two novel enhancers at the *HoxB* cluster locus are also required for RA-induced early ESC differentiation (80). Overall, these evidences reveal a direct regulatory relationship between enhancer and ESC lineage differentiation and highlight the important role of functional elements such as enhancer in fate determination of ESCs. However, we currently do not have a thorough understanding of the underlying mechanisms by which RA signaling promotes increased enhancer interactions. Recent studies employing using HiChIP technology reveal that mechanistically TFs function to regulate high-order chromatin structure and promote DNA-loop formation (81–83). Considering our previous results showing HOXA1 binding at the enhancer regions (En1 and En2), we therefore speculate that HOXA1 may be involved in regulating enhancer interactions, and these need further study.

Although lncRNAs reportedly regulate ESC multipotency, only a few studies report their orchestration of high-order chromatin structure in this context (27,33). *Halr1* (also known as *linc-HOXA1*, *Haunt*, *Gml5055* and *linc1547*) reportedly regulates *Hoxa1* expression in at least three ways: by binding PURB to transcriptionally repress *Hoxa1* (84), by binding to the PRC2 complex to mediate epigenetic repression (29), and by acting as a chromatin RNA to inhibit interaction of enhancers (here, En1 and En2) with *Hoxa1* chromatin (27). In this study, we focus on the regulatory effects of *Halr1* on chromatin structure (Figure 10D). By analyzing Hi-C and *Halr1*-ChIRP-DNA-seq data (8,27), we found that RA-induced high expression of *Halr1* binds mainly to the *Halr1-Hoxa1* locus and acts as a *cis*-acting element to regulate gene expression within a TAD (Supplementary Figure S10). Further by Capture-C screening, we found that deletion of *Halr1* not only facilitated the interactions of *Hoxa1* chromatin with enhancer En1 and En2 but also weakened the interactions with enhancer En3 and *HoxA* cluster (Figure 6). These results suggest that *Halr1* not only acts as a ‘brake’ to precisely control the interactions of *Hoxa1* chromatin with distal enhancers (27) but also acts as a ‘binder’ to maintain the interactions with enhancer and *HoxA* cluster. These results also suggest that *Halr1* RNA binds to the *HoxA* cluster as a chromatin RNA to maintain a relatively closed chromatin state and that in its absence, *HoxA* cluster chromatin becomes opened, allowing interaction with enhancers outside the cluster. Thus, these findings not only expand the role of *Halr1*'s function as a chromatin RNA but also further highlight the flexible nature of lncRNAs to regulate gene expression by orchestrating high-order chromatin structures.

Previous studies have shown that deletion of *Halr1* RNA significantly promotes the expression of *HoxA* cluster genes, while deletion of enhancer En1 significantly represses the expression of *HoxA* cluster genes, revealing the opposite regulation of *HoxA* cluster genes' expression by *Halr1* RNA

and its genomic locus, and our findings are consistent with that (27) (Supplementary Figure S14). Considering that we also found that HOXA1 promotes *Halr1* expression, together these results suggest a significant positive feedback regulation between *Hoxa1* and *Halr1* that may resemble a circular regulation. However, it is not clear who is the initiator of the regulation and this needs to be explored further (85). Furthermore, our transcriptome analysis reveals that *Halr1* regulates RA signaling-induced early ESC lineage differentiation particularly by promoting ESC endoderm differentiation, a novel role for *Halr1* not previously reported. Interestingly, we observed that *Halr1* was highly expressed in the early stage of spontaneous differentiation of ESCs (without LIF/2i). This pattern of expression of *Halr1* in early ESC differentiation is very similar to that of the previously reported lncRNA *Ephemerone* (86), a lncRNA expressed only in mouse ESCs. Unexpectedly, we found that *Halr1* is not present in human genome and is only expressed in the mouse. We also found significant differences in enhancer distribution and chromatin interactions at the *Skap2-Hoxa1* locus between mouse and human (Supplementary Figure S15) (8,63,87,88). These new findings suggest that *Halr1* is a species-specific lncRNA and may play other regulatory roles during early mouse ESC differentiation, which requires further investigation.

In conclusion, our studies reveal enhancer architecture-dependent multilayered transcriptional regulation at the *Halr1-Hoxa1* locus orchestrating RA signaling-induced early lineage differentiation of ESCs. These findings provide new insight into molecular mechanisms underlying ESC fate decisions.

DATA AVAILABILITY

The raw data produced in this study for the DNA-seq and RNA-seq data have been deposited in the National Center for Biotechnology Information (NCBI) Gene Expression Omnibus (GEO, <https://www.ncbi.nlm.nih.gov/geo/>) under the accession number GSE169058.

SUPPLEMENTARY DATA

Supplementary Data are available at NAR Online.

ACKNOWLEDGEMENTS

We thank all members of our laboratory for many helpful discussions. We also thank Dr Lingyi Chen (Professor, Nankai University), Dr Jun Zhou (Professor, Nankai University), Dr Xinyi Lu (Professor, Nankai University), Dr Jiayi Zhou (Professor, Chinese Academy of Medical Sciences) and Dr Weiping Yuan (Professor, Chinese Academy of Medical Sciences) for helpful comments. We also thank Dr Shaohui Chen for his comments during the early stage of this study. We also thank Dr Lamar for editing this article. *Author contributions:* W.L., G.S. and L.Z. conceived of and designed the study. W.L., G.S., L.Z., Z.Z. and J.S. supervised the study. G.S., X.Z., J.C., J.Z., M.L. and J.B. performed experiments and analyzed the data. W.W., S.S. and D.G. analyzed sequencing data. G.S., W.W. and B.C. performed bioinformatic analysis. G.S. and W.L. wrote the manuscript. All authors have read and approved the final manuscript.

FUNDING

National Key R&D Program of China [2017YFA0102600]; Fundamental Research Funds for the Central Universities (Nankai University) [63201087]. Funding for open access charge: National Key R&D Program of China [2017YFA0102600]; Fundamental Research Funds for the Central Universities (Nankai University) [63201087].
Conflict of interest statement. None declared.

REFERENCES

- Boyer, L.A., Lee, T.I., Cole, M.F., Johnstone, S.E., Levine, S.S., Zucker, J.P., Guenther, M.G., Kumar, R.M., Murray, H.L., Jenner, R.G. *et al.* (2005) Core transcriptional regulatory circuitry in human embryonic stem cells. *Cell*, **122**, 947–956.
- Young, R.A. (2011) Control of the embryonic stem cell state. *Cell*, **144**, 940–954.
- Zheng, H. and Xie, W. (2019) The role of 3D genome organization in development and cell differentiation. *Nat. Rev. Mol. Cell Biol.*, **20**, 535–550.
- Plasschaert, R.N., Vigneau, S., Tempera, I., Gupta, R., Maksimoska, J., Everett, L., Davuluri, R., Mamorstein, R., Lieberman, P.M., Schultz, D. *et al.* (2014) CTCF binding site sequence differences are associated with unique regulatory and functional trends during embryonic stem cell differentiation. *Nucleic Acids Res.*, **42**, 774–789.
- Wang, J., Huang, J. and Shi, G. (2020) Retrotransposons in pluripotent stem cells. *Cell Regener.*, **9**, 4.
- Ji, Z., Mohammed, H., Webber, A., Ridsdale, J., Han, N., Carroll, J.S. and Sharrocks, A.D. (2014) The forkhead transcription factor FOXK2 acts as a chromatin targeting factor for the BAP1-containing histone deubiquitinase complex. *Nucleic Acids Res.*, **42**, 6232–6242.
- Dixon, J.R., Jung, I., Selvaraj, S., Shen, Y., Antosiewicz-Bourget, J.E., Lee, A.Y., Ye, Z., Kim, A., Rajagopal, N., Xie, W. *et al.* (2015) Chromatin architecture reorganization during stem cell differentiation. *Nature*, **518**, 331–336.
- Bonev, B., Mendelson Cohen, N., Szabo, Q., Fritsch, L., Papadopoulos, G.L., Lubling, Y., Xu, X., Lv, X., Hugnot, J.P., Tanay, A. *et al.* (2017) Multiscale 3D genome rewiring during mouse neural development. *Cell*, **171**, 557–572.
- Osterwalder, M., Barozzi, I., Tissières, V., Fukuda-Yuzawa, Y., Mannion, B.J., Afzal, S.Y., Lee, E.A., Zhu, Y., Plajzer-Frick, I., Pickle, C.S. *et al.* (2018) Enhancer redundancy provides phenotypic robustness in mammalian development. *Nature*, **554**, 239–243.
- Mead, T.J., Wang, Q., Bhattaram, P., Dy, P., Afelik, S., Jensen, J. and Lefebvre, V. (2013) A far-upstream (-70 kb) enhancer mediates Sox9 auto-regulation in somatic tissues during development and adult regeneration. *Nucleic Acids Res.*, **41**, 4459–4469.
- Wei, Z., Gao, F., Kim, S., Yang, H., Lyu, J., An, W., Wang, K. and Lu, W. (2013) Klf4 organizes long-range chromosomal interactions with the oct4 locus in reprogramming and pluripotency. *Cell Stem Cell*, **13**, 36–47.
- Das, B.C., Thapa, P., Karki, R., Das, S., Mahapatra, S., Liu, T.C., Torregroza, I., Wallace, D.P., Kambhampati, S., Van Veldhuizen, P. *et al.* (2014) Retinoic acid signaling pathways in development and diseases. *Development*, **22**, 673–683.
- Erkelens, M.N. and Mebius, R.E. (2017) Retinoic acid and immune homeostasis: a balancing act. *Trends Immunol.*, **38**, 168–180.
- Das, B.C., Thapa, P., Karki, R., Das, S., Mahapatra, S., Liu, T.C., Torregroza, I., Wallace, D.P., Kambhampati, S., Van Veldhuizen, P. *et al.* (2014) Retinoic acid signaling pathways in development and diseases. *Bioorg. Med. Chem.*, **22**, 673–683.
- Ablain, J. and de Thè, H. (2014) Retinoic acid signaling in cancer: the parable of acute promyelocytic leukemia. *Int. J. Cancer*, **135**, 2262–2272.
- Chatagnon, A., Veber, P., Morin, V., Bedo, J., Triqueneaux, G., Semon, M., Laudet, V., Buc, F. and Benoit, G. (2015) RAR/RXR binding dynamics distinguish pluripotency from differentiation associated cis-regulatory elements. *Nucleic Acids Res.*, **43**, 4833–4854.
- Simandi, Z., Horvath, A., Wright, L.C., Cuaranta-Monroy, I., De Luca, I., Karolyi, K., Sauer, S., Deleuze, J.F., Gudas, L.J., Cowley, S.M. *et al.* (2016) OCT4 Acts as an integrator of pluripotency and signal-induced differentiation. *Mol. Cell*, **63**, 647–661.
- De Kumar, B., Parker, H.J., Parrish, M.E., Lange, J.J., Slaughter, B.D., Unruh, J.R., Paulson, A. and Krumlauf, R. (2017) Dynamic regulation of Nanog and stem cell-signaling pathways by Hoxa1 during early neuro-ectodermal differentiation of ES cells. *PNAS*, **114**, 5838–5845.
- De Kumar, B., Parker, H.J., Paulson, A., Parrish, M.E., Zeitlinger, J. and Krumlauf, R. (2017) Hoxa1 targets signaling pathways during neural differentiation of ES cells and mouse embryogenesis. *Dev. Biol.*, **432**, 151–164.
- Martinez-Ceballos, E. and Gudas, L.J. (2008) Hoxa1 is required for the retinoic acid-induced differentiation of embryonic stem cells into neurons. *J. Neurosci. Res.*, **86**, 2809–2819.
- De Kumar, B., Parker, H.J., Paulson, A., Parrish, M.E., Pushel, I., Singh, N.P., Zhang, Y., Slaughter, B.D., Unruh, J.R., Florens, L. *et al.* (2017) HOXA1 and TALE proteins display cross-regulatory interactions and form a combinatorial binding code on HOXA1 targets. *Genome Res.*, **27**, 1501–1512.
- Kubo, N., Ishii, H., Xiong, X., Bianco, S., Meitinger, F., Hu, R., Hocker, J.D., Conte, M., Gorkin, D., Yu, M. *et al.* (2021) Promoter-proximal CTCF binding promotes distal enhancer-dependent gene activation. *Nat. Struct. Mol. Biol.*, **28**, 152–161.
- Su, G., Wang, W., Chen, J., Liu, M., Zheng, J., Guo, D., Bi, J., Zhao, Z., Shi, J., Zhang, L. *et al.* (2021) CTCF-binding element regulates ESC differentiation via orchestrating long-range chromatin interaction between enhancers and HoxA. *J. Biol. Chem.*, **296**, 100413.
- Narendra, V., Rocha, P.P., An, D., Raviram, R., Skok, J.A., Mazzone, E.O. and Reinberg, D. (2015) CTCF establishes discrete functional chromatin domains at the Hox clusters during differentiation. *Science*, **347**, 1017–1021.
- Capo-Chichi, C.D., Rula, M.E., Smedberg, J.L., Vanderveer, L., Parmacek, M.S., Morrisey, E.E., Godwin, A.K. and Xu, X.X. (2005) Perception of differentiation cues by GATA factors in primitive endoderm lineage determination of mouse embryonic stem cells. *Dev. Biol.*, **286**, 574–586.
- Su, G., Guo, D., Chen, J., Liu, M., Zheng, J., Wang, W., Zhao, X., Yin, Q., Zhang, L., Zhao, Z. *et al.* (2019) A distal enhancer maintaining Hoxa1 expression orchestrates retinoic acid-induced early ESCs differentiation. *Nucleic Acids Res.*, **47**, 6737–6752.
- Yin, Y., Yan, P., Lu, J., Song, G., Zhu, Y., Li, Z., Zhao, Y., Shen, B., Huang, X., Zhu, H. *et al.* (2015) Opposing roles for the lncRNA haunt and its genomic locus in regulating HOXA gene activation during embryonic stem cell differentiation. *Cell Stem Cell*, **16**, 504–516.
- Cao, K., Collings, C.K., Marshall, S.A., Morgan, M.A., Rendleman, E.J., Wang, L., Sze, C.C., Sun, T., Bartom, E.T. and Shilatifard, A. (2017) SET1A/COMPASS and shadow enhancers in the regulation of homeotic gene expression. *Genes Dev.*, **31**, 787–801.
- Liu, G.Y., Zhao, G.N., Chen, X.F., Hao, D.L., Zhao, X., Lv, X. and Liu, D.P. (2016) The long noncoding RNA Gm15055 represses Hoxa gene expression by recruiting PRC2 to the gene cluster. *Nucleic Acids Res.*, **44**, 2613–2627.
- Acharya, D., Hainer, S.J., Yoon, Y., Wang, F., Bach, I., Rivera-Pérez, J.A. and Fazio, T.G. (2017) KAT-independent gene regulation by Tip60 promotes ESC self-renewal but not pluripotency. *Cell Rep.*, **19**, 671–679.
- Schmittgen, T.D. and Livak, K.J. (2008) Analyzing real-time PCR data by the comparative C(T) method. *Nat. Protoc.*, **3**, 1101–1108.
- Li, P., Ding, N., Zhang, W. and Chen, L. (2018) COPS2 antagonizes OCT4 to accelerate the G2/M transition of mouse embryonic stem cells. *Stem cell reports*, **11**, 317–324.
- Zhao, T., Cai, M., Liu, M., Su, G., An, D., Moon, B., Lyu, G., Si, Y., Chen, L. and Lu, W. (2020) lncRNA 5430416N02Rik promotes the proliferation of mouse embryonic stem cells by activating Mid1 expression through 3D chromatin architecture. *Stem cell reports*, **14**, 493–505.
- Cong, L., Ran, F.A., Cox, D., Lin, S., Barretto, R., Habib, N., Hsu, P.D., Wu, X., Jiang, W., Marraffini, L.A. *et al.* (2013) Multiplex genome engineering using CRISPR/Cas systems. *Science*, **339**, 819–823.
- Davies, J.O., Telenius, J.M., McGowan, S.J., Roberts, N.A., Taylor, S., Higgs, D.R. and Hughes, J.R. (2016) Multiplexed analysis of chromosome conformation at vastly improved sensitivity. *Nat. Methods*, **13**, 74–80.

36. Hughes, J.R., Roberts, N., McGowan, S., Hay, D., Giannoulou, E., Lynch, M., De Gobbi, M., Taylor, S., Gibbons, R. and Higgs, D.R. (2014) Analysis of hundreds of cis-regulatory landscapes at high resolution in a single, high-throughput experiment. *Nat. Genet.*, **46**, 205–212.
37. Angiuoli, S.V. and Salzberg, S.L. (2011) Mugsy: fast multiple alignment of closely related whole genomes. *Bioinformatics*, **27**, 334–342.
38. Freese, N.H., Norris, D.C. and Loraine, A.E. (2016) Integrated genome browser: visual analytics platform for genomics. *Bioinformatics*, **32**, 2089–2095.
39. Zhou, X., Lowdon, R.F., Li, D., Lawson, H.A., Madden, P.A., Costello, J.F. and Wang, T. (2013) Exploring long-range genome interactions using the WashU Epigenome Browser. *Nat. Methods*, **10**, 375–376.
40. Anders, S., Pyl, P.T. and Huber, W. (2015) HTSeq—a Python framework to work with high-throughput sequencing data. *Bioinformatics*, **31**, 166–169.
41. Love, M.I., Huber, W. and Anders, S. (2014) Moderated estimation of fold change and dispersion for RNA-seq data with DESeq2. *Genome Biol.*, **15**, 550.
42. Zhou, Y., Zhou, B., Pache, L., Chang, M., Khodabakhshi, A.H., Tanaseichuk, O., Benner, C. and Chanda, S.K. (2019) Metascape provides a biologist-oriented resource for the analysis of systems-level datasets. *Nat. Commun.*, **10**, 1523.
43. Huang, D.W., Sherman, B.T. and Liempicki, R.A. (2009) Systematic and integrative analysis of large gene lists using DAVID bioinformatics resources. *Nat. Protoc.*, **4**, 44–57.
44. Subramanian, A., Tamayo, P., Mootha, V.K., Mukherjee, S., Ebert, B.L., Gillette, M.A., Paulovich, A., Pomeroy, S.L., Golub, T.R., Lander, E.S. *et al.* (2005) Gene set enrichment analysis: a knowledge-based approach for interpreting genome-wide expression profiles. *PNAS*, **102**, 15545–15550.
45. Mootha, V.K., Lindgren, C.M., Eriksson, K.F., Subramanian, A., Sihag, S., Lehar, J., Puigserver, P., Carlsson, E., Ridderstråle, M., Laurila, E. *et al.* (2003) PGC-1 α -responsive genes involved in oxidative phosphorylation are coordinately downregulated in human diabetes. *Nat. Genet.*, **34**, 267–273.
46. Kanehisa, M., Sato, Y., Kawashima, M., Furumichi, M. and Tanabe, M. (2016) KEGG as a reference resource for gene and protein annotation. *Nucleic Acids Res.*, **44**, D457–D462.
47. Wang, Y., Song, F., Zhang, B., Zhang, L., Xu, J., Kuang, D., Li, D., Choudhary, M.N.K., Li, Y., Hu, M. *et al.* (2018) The 3D Genome Browser: a web-based browser for visualizing 3D genome organization and long-range chromatin interactions. *Genome Biol.*, **19**, 151.
48. Mei, S., Qin, Q., Wu, Q., Sun, H., Zheng, R., Zang, C., Zhu, M., Wu, J., Shi, X., Taing, L. *et al.* (2017) Cistrome Data Browser: a data portal for ChIP-Seq and chromatin accessibility data in human and mouse. *Nucleic Acids Res.*, **45**, D658–D662.
49. Zheng, R., Wan, C., Mei, S., Qin, Q., Wu, Q., Sun, H., Chen, C.H., Brown, M., Zhang, X., Meyer, C.A. *et al.* (2019) Cistrome Data Browser: expanded datasets and new tools for gene regulatory analysis. *Nucleic Acids Res.*, **47**, D729–D735.
50. Zhang, P., Andrianakos, R., Yang, Y., Liu, C. and Lu, W. (2010) Kruppel-like factor 4 (Klf4) prevents embryonic stem (ES) cell differentiation by regulating Nanog gene expression. *J. Biol. Chem.*, **285**, 9180–9189.
51. Moutier, E., Ye, T., Choukallah, M.A., Urban, S., Osz, J., Chatagnon, A., Delacroix, L., Langer, D., Rochel, N., Moras, D. *et al.* (2012) Retinoic acid receptors recognize the mouse genome through binding elements with diverse spacing and topology. *J. Biol. Chem.*, **287**, 26328–26341.
52. Costa-Giomi, M.P., Gaub, M.P., Chambon, P. and Abarzúa, P. (1992) Characterization of a retinoic acid responsive element isolated by whole genome PCR. *Nucleic Acids Res.*, **20**, 3223–3232.
53. Loudig, O., Babichuk, C., White, J., Abu-Abed, S., Mueller, C. and Petkovich, M. (2000) Cytochrome P450RAI (CYP26) promoter: a distinct composite retinoic acid response element underlies the complex regulation of retinoic acid metabolism. *Mol. Endocrinol.*, **14**, 1483–1497.
54. Huang, D., Chen, S.W. and Gudas, L.J. (2002) Analysis of two distinct retinoic acid response elements in the homeobox gene *Hoxb1* in transgenic mice. *Dev. Dyn.*, **223**, 353–370.
55. Huang, D., Chen, S.W., Langston, A.W. and Gudas, L.J. (1998) A conserved retinoic acid responsive element in the murine *Hoxb-1* gene is required for expression in the developing gut. *Development*, **125**, 3235–3246.
56. Marshall, H., Studer, M., Pöpperl, H., Aparicio, S., Kuroiwa, A., Brenner, S. and Krumlauf, R. (1994) A conserved retinoic acid response element required for early expression of the homeobox gene *Hoxb-1*. *Nature*, **370**, 567–571.
57. Nolte, C., Jinks, T., Wang, X., Martinez Pastor, M.T. and Krumlauf, R. (2013) Shadow enhancers flanking the *HoxB* cluster direct dynamic *Hox* expression in early heart and endoderm development. *Dev. Biol.*, **383**, 158–173.
58. Studer, M., Pöpperl, H., Marshall, H., Kuroiwa, A. and Krumlauf, R. (1994) Role of a conserved retinoic acid response element in rhombomere restriction of *Hoxb-1*. *Science*, **265**, 1728–1732.
59. Kim, M.H., Shin, J.S., Park, S., Hur, M.W., Lee, M.O., Park, H. and Lee, C.S. (2002) Retinoic acid response element in *HOXA-7* regulatory region affects the rate, not the formation of anterior boundary expression. *Int. J. Dev. Biol.*, **46**, 325–328.
60. Fornes, O., Castro-Mondragon, J.A., Khan, A., van der Lee, R., Zhang, X., Richmond, P.A., Modi, B.P., Correard, S., Gheorghe, M., Baranašić, D. *et al.* (2020) JASPAR 2020: update of the open-access database of transcription factor binding profiles. *Nucleic Acids Res.*, **48**, D87–D92.
61. Qian, Y., Zhang, L., Cai, M., Li, H., Xu, H., Yang, H., Zhao, Z., Rhie, S.K., Farnham, P.J., Shi, J. *et al.* (2019) The prostate cancer risk variant rs55958994 regulates multiple gene expression through extreme long-range chromatin interaction to control tumor progression. *Sci. Adv.*, **5**, eaaw6710.
62. Kempfer, R. and Pombo, A. (2020) Methods for mapping 3D chromosome architecture. *Nat. Rev. Genet.*, **21**, 207–226.
63. Xiao, S., Xie, D., Cao, X., Yu, P., Xing, X., Chen, C.C., Musselman, M., Xie, M., West, F.D., Lewin, H.A. *et al.* (2012) Comparative epigenomic annotation of regulatory DNA. *Cell*, **149**, 1381–1392.
64. Wang, K.C. and Chang, H.Y. (2011) Molecular mechanisms of long noncoding RNAs. *Mol. Cell*, **43**, 904–914.
65. Mercer, T.R. and Mattick, J.S. (2013) Structure and function of long noncoding RNAs in epigenetic regulation. *Nat. Struct. Mol. Biol.*, **20**, 300–307.
66. Yang, Y.W., Flynn, R.A., Chen, Y., Qu, K., Wan, B., Wang, K.C., Lei, M. and Chang, H.Y. (2014) Essential role of lncRNA binding for WDR5 maintenance of active chromatin and embryonic stem cell pluripotency. *eLife*, **3**, e02046.
67. Burton, A. and Torres-Padilla, M.E. (2014) Chromatin dynamics in the regulation of cell fate allocation during early embryogenesis. *Nat. Rev. Mol. Cell Biol.*, **15**, 723–734.
68. Hsieh, T.S., Cattoglio, C., Slobodyanyuk, E., Hansen, A.S., Rando, O.J., Tjian, R. and Darzacq, X. (2020) Resolving the 3D landscape of transcription-linked mammalian chromatin folding. *Mol. Cell*, **78**, 539–553.
69. Nair, L., Chung, H. and Basu, U. (2020) Regulation of long non-coding RNAs and genome dynamics by the RNA surveillance machinery. *Nature reviews. Mol. Cell Biol.*, **21**, 123–136.
70. Ying, Q.L., Wray, J., Nichols, J., Batlle-Morera, L., Doble, B., Woodgett, J., Cohen, P. and Smith, A. (2008) The ground state of embryonic stem cell self-renewal. *Nature*, **453**, 519–523.
71. Huang, G., Ye, S., Zhou, X., Liu, D. and Ying, Q.L. (2015) Molecular basis of embryonic stem cell self-renewal: from signaling pathways to pluripotency network. *Cell. Mol. Life Sci.: CMLS*, **72**, 1741–1757.
72. De Felice, M., Falco, G., Wang, Y., Na, Q., Li, X., Tee, W.W. and Wu, B. (2021) Retinoic acid induces NELFA-mediated 2C-like state of mouse embryonic stem cells associates with epigenetic modifications and metabolic processes in chemically defined media. *Cell Death Differ.*, **54**, e13049.
73. Tagliaferri, D., Mazzone, P., Noviello, T.M.R., Addeo, M., Angrisano, T., Del Vecchio, L., Visconte, F., Ruggieri, V., Russi, S., Caivano, A. *et al.* (2019) Retinoic acid induces embryonic stem cells (ESCs) Transition to 2 Cell-Like state through a coordinated expression of *dux* and *duxbl1*. *Front. Cell Dev. Biol.*, **7**, 385.
74. Iturbide, A., Ruiz Tejada Segura, M.L., Noll, C., Schorpp, K., Rothenaigner, I., Ruiz-Morales, E.R., Lubatti, G., Agami, A., Hadian, K., Scialdone, A. *et al.* (2021) Retinoic acid signaling is critical during the totipotency window in early mammalian development. *Nat. Struct. Mol. Biol.*, **28**, 521–532.

75. Wang, Y., Na, Q., Li, X., Tee, W.-W., Wu, B. and Bao, S. (2021) Retinoic acid induces NELFA-mediated 2C-like state of mouse embryonic stem cells associates with epigenetic modifications and metabolic processes in chemically defined media. *Cell Prolif.*, **54**, e13049.
76. Tsankov, A.M., Gu, H., Akopian, V., Ziller, M.J., Donaghey, J., Amit, I., Gnirke, A. and Meissner, A. (2015) Transcription factor binding dynamics during human ES cell differentiation. *Nature*, **518**, 344–349.
77. Ji, Z., Li, Y., Liu, S.X. and Sharrocks, A.D. (2021) The forkhead transcription factor FOXK2 premarks lineage-specific genes in human embryonic stem cells for activation during differentiation. *Nucleic Acids Res.*, **49**, 1345–1363.
78. Dupé, V., Davenne, M., Brocard, J., Dollé, P., Mark, M., Dierich, A., Chambon, P. and Rijli, F.M. (1997) In vivo functional analysis of the Hoxa-1 3' retinoic acid response element (3'RARE). *Development*, **124**, 399–410.
79. Langston, A.W., Thompson, J.R. and Gudas, L.J. (1997) Retinoic acid-responsive enhancers located 3' of the Hox A and Hox B homeobox gene clusters. Functional analysis. *J. Biol. Chem.*, **272**, 2167–2175.
80. Zheng, J., Su, G., Wang, W., Zhao, X., Liu, M., Bi, J., Zhao, Z., Shi, J., Lu, W. and Zhang, L. (2021) Two enhancers regulate HoxB genes expression during retinoic acid-induced early embryonic stem cells differentiation through long-range chromatin interactions. *Stem Cells Dev.*, **30**, 683–695.
81. Chen, L., Cao, W., Aita, R., Aldea, D., Flores, J., Gao, N., Bonder, E.M., Ellison, C.E. and Verzi, M.P. (2021) Three-dimensional interactions between enhancers and promoters during intestinal differentiation depend upon HNF4. *Cell Rep.*, **34**, 108679.
82. Rowley, M.J., Nichols, M.H., Lyu, X., Ando-Kuri, M., Rivera, I.S.M., Hermetz, K., Wang, P., Ruan, Y. and Corces, V.G. (2017) Evolutionarily conserved principles predict 3D chromatin organization. *Mol. Cell*, **67**, 837–852.
83. Cai, W., Huang, J., Zhu, Q., Li, B.E., Seruggia, D., Zhou, P., Nguyen, M., Fujiwara, Y., Xie, H., Yang, Z. *et al.* (2020) Enhancer dependence of cell-type-specific gene expression increases with developmental age. *Proc. Natl. Acad. Sci. U.S.A.*, **117**, 21450–21458.
84. Maamar, H., Cabili, M.N., Rinn, J. and Raj, A. (2013) linc-HOXA1 is a noncoding RNA that represses Hoxa1 transcription in cis. *Genes Dev.*, **27**, 1260–1271.
85. Lin, N., Dang, J. and Rana, T.M. (2015) Haunting the HOXA locus: two faces of lncRNA regulation. *Cell stem cell*, **16**, 449–450.
86. Li, M.A., Amaral, P.P., Cheung, P., Bergmann, J.H., Kinoshita, M., Kalkan, T., Ralser, M., Robson, S., von Meyenn, F., Paramor, M. *et al.* (2017) A lncRNA fine tunes the dynamics of a cell state transition involving Lin28, let-7 and de novo DNA methylation. *eLife*, **6**, e23468.
87. Zhang, Y., Li, T., Preissl, S., Amaral, M.L., Grinstein, J.D., Farah, E.N., Destici, E., Qiu, Y., Hu, R., Lee, A.Y. *et al.* (2019) Transcriptionally active HERV-H retrotransposons demarcate topologically associating domains in human pluripotent stem cells. *Nat. Genet.*, **51**, 1380–1388.
88. Rada-Iglesias, A., Bajpai, R., Swigut, T., Brugmann, S.A., Flynn, R.A. and Wysocka, J. (2011) A unique chromatin signature uncovers early developmental enhancers in humans. *Nature*, **470**, 279–283.